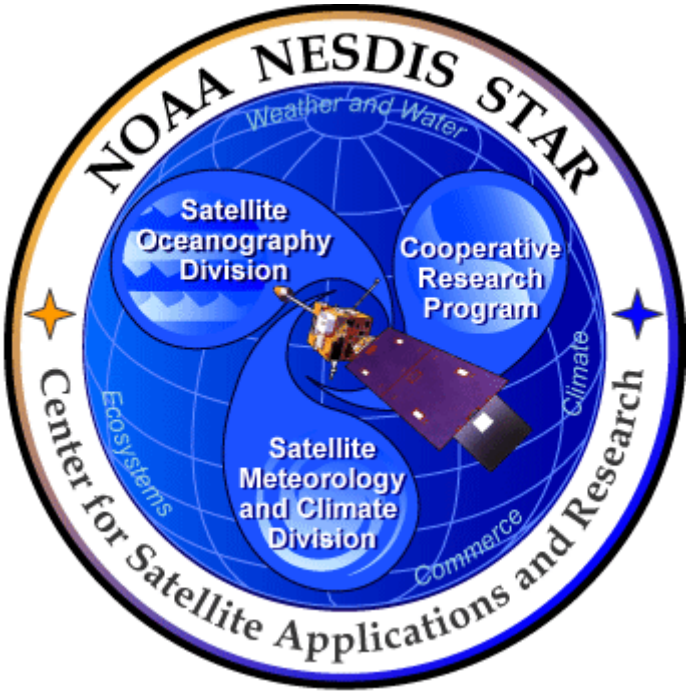

NOAA NESDIS
CENTER for SATELLITE APPLICATIONS and RESEARCH

GOES-R Advanced Baseline Imager (ABI) Algorithm Theoretical Basis Document For Surface Albedo

Yunyue Yu, Jingjing Peng, Lei Ji, Peng Yu, NOAA/NESDIS/STAR

Version 4
Mar 2024

VERSION HISTORY SUMMARY

Version	Description	Revised Sections	Date
0.1	New ATBD Document according to NOAA /NESDIS/STAR Document Guideline		8/30/2008
0.2	GOES-R Advanced Baseline Imager (ABI) Algorithm Theoretical Basis Document for Surface Albedo		9/30/2008
1.0	ATBD Document 80% readiness	Adding discussions on product uses in Section 2; Updating the newly developed algorithm in Section3; Providing validation results in Section 4; Supplementing more details in Sections 5 & 6	6/30/2010
2.0	ATBD Document 100% readiness	Describing the back-up algorithm; adding details on different paths to calculate BRF; providing graceful degradation strategies; updating with more validation results	6/12/2011
2.1	Corresponding to code version 6.0	Correcting and updating some information	12/1/2016
2.2	Corresponding to code version 7.0	Updating some information for QC and online processing outline	3/14/2017
2.2.1	Corresponding to code version 7.0	Correcting and updating some information	4/5/2017
2.2.2	Corresponding to code version 7.1	Add the startup setup and interruption control section; Updated the monitoring metadata list	2/22/2018
2.2.3	Corresponding to code version 7.1	Updated the metadata list and input instruction	3/23/2018
2.2.4	Corresponding to code version 7.2	Updated the description in Startup processing	04/12/2018
2.2.5	Corresponding to code version 7.3	Updated the description in Startup processing	05/20/2018
3	Corresponding to Framework code version v2r0 (The first integrated version in the operational system.	Main updates include the cloud screening and subroutine selection criteria in online process, and BRDF calibration by integrating BRDF climatology in offline optimization.	09/20/2020
3.1	Corresponding to Ground System code Enterprise version (and the L2 product).	Online algorithm improvement including the atmospheric LUTs and subroutine definition. Updated the validation	08/31/2021
4	Corresponding to DAP v3	Add NBAR as output parameter; updated all Quality Flag definition	03/31/2024
4.1	Corresponding to DAP v3	Updated the latest sample output and validation results	7/27/2025

TABLE OF CONTENTS

Page

● LIST OF FIGURES

Page

● LIST OF TABLES

● LIST OF ACRONYMS

2D	Two Dimension
ABI	Advanced Baseline Imager
ACM	ABI Cloud Mask
AIT	Algorithm Integration Team
AOD	Aerosol Optical Depth
ASTER	Advanced Spaceborne Thermal Emission and Reflection Radiometer
ATBD	Algorithm Theoretical Base Document
AVHRR	Advanced Very High-Resolution Radiometer
BRDF	Bidirectional Reflectance Distribution Function
BRF	Bidirectional Reflectance Factor, refer to Surface Reflectance hereafter
ETM+	Enhanced Thematic Mapper Plus
FD	Full Disk
FPT	Focal Plane Temperature
GOES	Geostationary Operational Environmental Satellite
GS-F&PS	Ground Segment Functional and Performance Specification
L1B	Level 1B
LSA	Land Surface Albedo
LUT	Look Up Table
LZA	Local Zenith Angle
MFRSR	Multi-Filter Rotating Shadowband Radiometers
MISR	Multi-angle Imaging Spectroradiometer
MODIS	Moderate Resolution Imaging Spectroradiometer
MRD	Mission Requirement Document
MSG	Meteosat Second Generation
NCEP	National center for Environmental Prediction
NESDIS	National Environmental Satellite, Data, and Information Service
NOAA	National Oceanic and Atmospheric Administration
OLI	Operational Land Imager (OLI)
PAR	Photosynthetically Active Radiation
POLDER	Polarization and Directionality of the Earth's Reflectance
PQI	Product Quality Information
PSP	Precision Spectral Pyranometer
QF	Quality Flag
QC	Quality Control
SEVIRI	Spanning Enhanced Visible and Infrared Imager
SNR	Signal Noise Ratio
SPOT	Systeme pour l'Observation de la Terre
STAR	Center for Satellite Applications and Research
SURFRAD	SURFace RADiation network
SZA	Solar Zenith Angle
TOA	Top Of Atmosphere
UTC	Coordinated Universal Time
VIIRS	Visible/Infrared Imager /Radiometer Suite

ABSTRACT

This land surface albedo (LSA) Algorithm Theoretical Basis Document (ATBD) provides a high-level description and the physical and theoretical basis for the estimation of LSA with images taken by Advanced Baseline Imager (ABI) onboard the Geostationary Environmental Operational Satellite (GOES) R and S series of National Oceanic and Atmospheric Administration (NOAA) geostationary meteorological satellites. LSA is defined as the ratio between outgoing and incoming irradiance at the earth surface, which is a key component of surface energy budget. Besides the blue-sky broadband shortwave albedo, the LSA algorithm also generates spectral land surface reflectance as byproducts. The frequent temporal refreshment, fine spectral resolution and large spatial coverage make ABI a unique data source for mapping LSA. The ABI LSA algorithm combines atmospheric correction and surface Bidirectional Reflectance Distribution Function (BRDF) modeling in one optimization step to estimate BRDF parameters for each band. To improve computational efficiency, the ABI LSA algorithm is separated into the offline mode and the online mode. The routine offline mode is carried out at the end of each day, using a time series of clear-sky observations up to the current day to estimate BRDF parameters for the next days' online mode. In the online mode, LSA and surface reflectance products are produced in real-time. The direct estimation approach of albedo is implemented as the back-up algorithm when the routine offline algorithm fails. The ABI LSA algorithm has been tested and validated using satellite data. Comparison with field measurements shows our algorithm can satisfy the requirements of the GOES-R Ground Segment Functional and Performance Specification (F&PS).

1 INTRODUCTION

The purpose, users, scope, related documents and revision history of this document are briefly described in this section. Section 2 gives an overview of the Advanced Baseline Imager (ABI) Land Surface Albedo (LSA) algorithm derivation objectives and operation concept. Section 3 describes the LSA algorithm, its input data requirements, the theoretical background, mathematical descriptions and output of the algorithm. Some test results will be presented in Section 4. Practical considerations are described in Section 5 and followed by Section 6 on assumptions and limitations. Finally, Section 7 presents the references cited.

1.1 Purpose of This Document

The LSA Algorithm Theoretical Basis Document (ATBD) provides a high level description and the physical basis for the estimation of land surface albedo with images taken by ABI onboard the Geostationary Environmental Operational Satellite (GOES) R and S series of NOAA geostationary meteorological satellites. The LSA is a key parameter controlling surface radiation and energy budgets. LSA and land surface reflectance are also needed by other algorithms, such as snow coverage and radiation flux products.

1.2 Who Should Use This Document

The intended users of this document are those interested in understanding the physical basis of the algorithms and how to use the output of this algorithm to optimize the albedo estimate for a particular application. This document also provides information useful to anyone maintaining or modifying the original algorithm.

1.3 Inside Each Section

This document is subdivided into the following main sections:

- **System Overview**: Provides relevant details of the ABI and a brief description of the products generated by the algorithm.

- **Algorithm Description**: Provides a detailed description of the algorithm including its physical basis, its input, and its output.

- **Test Data Sets and Output**: Provides a description of the test data sets for characterizing the performance of the algorithm and quality of the data products. It also describes the results from algorithm processing using simulated input data.

- **Practical Considerations**: Provides an overview of the issues involving in numerical computation, programming and procedures, quality assessment and diagnostics and exception handling.

- **Assumptions and Limitations**: Provides an overview of the current limitations of the approach and gives the plan for overcoming these limitations with further algorithm development.

1.4 BRF and BRDF

Bidirectional reflectance factor (BRF) and bidirectional reflectance distribution function (BRDF) are two concepts that will be used frequently in this document. BRF is one kind of reflectance, a ratio between outgoing radiance at one given direction and incoming radiance at another given direction (same or different from the incoming direction). The reflectance byproduct of the LSA algorithm is the product of BRF. Surface reflectance and BRF are used interchangeably in this document. BRDF is a model to describe the bi-directional properties of reflectivity. In this document, BRDF is also used in the term "BRDF parameters" to refer to the kernel coefficients of the BRDF model.

1.5 Related Documents

LSA is one product of ABI product streamlines. The requirements of LSA products can be found in the specifications of the GOES-R Ground Segment Functional and Performance Specification (F&PS). LSA also requires other ABI products as the algorithm input. The readers can refer to these specific ATBDs for more information:

- *GOES-R Algorithm Theoretical Base Document for ABI Aerosol Optical Depth*
- *GOES-R Algorithm Theoretical Base Document for ABI Cloud Mask*

More references about the algorithm details are given in Section 5.

1.6 Revision History

Version 0.2 of this document was created by Drs. Shunlin Liang and Kaicun Wang of the Department of Geographical Science, University of Maryland, College Park and Dr. Yunyue Yu of NOAA NESDIS, Center for Satellite Applications and Research, Camp Springs, Maryland. According to the reviewers' comments, version of 1.0 was updated by Drs. Shunlin Liang and Dongdong Wang of the Department of Geographical Science, University of Maryland, College Park, and Dr. Yunyue Yu of NOAA. Refinement of the algorithm and latest validation results are updated in the Version 2.2 by Drs. Shunlin Liang, Dongdong Wang, Tao He and Mr. Yi Zhang of the Department of Geographical Science, University of Maryland, College Park, and Dr. Yunyue Yu of NOAA. Sartup set up and interruption control, metadata list and input data control are updated in the version 2.2 by Dr. Yunyue Yu of NOAA, and Dr. Jingjing Peng of the Earth System Science Interdisciplinary Center, University of Maryland, College Park. In response of the snow fraction user feedback to revise the snow reflectance and failure of albedo test in radiation product, the online process and offline algorithm improved in version 3 was updated by Dr. Jingjing Peng and Dr. Yunyue Yu of NOAA of the Earth System Science Interdisciplinary Center, University of Maryland, College Park. According to the algorithm redesign, output improvement, online algorithm calibration in LUTs, implementation in Ground System, comprehensive validation for provisional review, the version 3.1 and version 4 was updated by Dr. Jingjing Peng, Dr. Yunyue Yu, and Dr. Peng Yu of NOAA of the Earth System Science Interdisciplinary Center, University of Maryland, College Park. Meanwhile, the product has been declared of provisional maturity.

2 OBSERVING SYSTEM OVERVIEW

This section describes the products generated by the ABI LSA algorithm and the requirements it places on the sensor.

2.1 Products Generated

This albedo algorithm is responsible for estimation of LSA and land surface BRF over land surface. This algorithm estimates AOD with atmospheric parameters together, and then retrieves the parameters of the land surface BRDF model and derive LSA. Land surface reflectance values is estimated through atmospheric correction using the ABI Aerosol Optical Depth (AOD) product or AOD climatology. The albedo algorithm also incorporates albedo climatology and BRDF climatology from previous satellite products (MODIS) as prior knowledge. Full disk blue-sky broadband albedo for the solar zenith angle smaller than 67° is produced. As a byproduct, full disk surface BRFs at the five visible and near-infrared bands are generated as well.

The surface albedo/reflectance product requirements defined by the Mission Requirement Document (MRD) and the Ground Segment Functional and Performance Specification (GS-F&PS) (NOAA 2009) are listed in Tables 2.1 and 2.2.

Table 2.1. GOES-R mission requirements for LSA (a) and BRF (b) products

(a)

Observational Requirement	Geographic Coverage[2]	Horiz. Res.	Mapping Accuracy	Msmnt. Range (albedo unit)	Msmnt. Accuracy (albedo unit)	Msmnt. Precision	Refresh Rate	Data Latency	Long-term Stability	Exent Qualifier
Albedo: Full Disk	FD	2 km	2 km	0 to 1	0.08	10%	10 mins	<2000 secs	TBD	LZA <70

(b)

Observational Requirement	Geographic Coverage[2]	Horiz. Res.	Mapping Accuracy	Msmnt. Range	Msmnt. cAccuray	Msmnt. Precision	Refresh Rate	Data Latency	Long-term Stability	Extent Qualifier
Reflectance: Full Disk	FD	2 km	2 km	0 to 2	0.08	0.08	10 mins	<2000 secs	TBD	LZA <70

As the key component of surface energy budget, satellite albedo products can be used to drive/calibrate/validate climatic, mesoscale atmospheric, hydrological and land surface models. Variation of LSA is also an important indicator of land cover and land use change. Analysis of long-term reliable albedo products will help better understand the human dimension of climate change and how the vegetation-albedo-climate feedback work.

Table 2.2. lists the frequency of each scan type for Modes 4 and 6. It includes the cadence of the operational LSA/BRF product. The bottom line reflects, for each appropriate scan type, the frequency of that product used for verification purposes.

Table 2.2. LSA/BRF product cadence

Mode	Mode 4			Mode 6		
Scan Type	FD	CONUS	Mesoscale	FD	CONUS	Mesoscale
Scan Freq	5 min	5 min*	N/A	10 min	5 min	30 sec^
LSA/BRF Output	10 min	5 min	N/A	10 min	5 min	1 min
Verify Freq	Random sampling	Random sampling	N/A	Random sampling	Random sampling	Random sampling

** There is no CONUS scan type for Mode 4, but there are required products over the CONUS that are derived from the FD output*

^ The refresh rate for mesoscale products applies to each of the two mesoscale scenes in the ABI Mode 6 epoch. A 30 second refresh rate is provided if the two mesoscale scenes are geographically coincident. Otherwise, the refresh rate is 60 seconds.

2.2 *Instrument Characteristics*

The LSA product is produced from clear-sky pixels observed by the ABI. The final channel set is still being determined as the algorithms are developed and validated. Table 2.3 highlights the ABI channels used by the albedo algorithm.

Table 2.3 Spectral characteristics of Advanced Baseline Imager

Channel Number	Central Wavelength (μm)	Bandwidth (μm)	Spatial Resolution
1	0.47	0.45 – 0.49	1 km
2	0.64	0.59 – 0.69	0.5 km
3	0.86	0.85– 0.89	1 km
5	1.61	1.58 – 1.64	1 km
6	2.26	2.23 – 2.28	2 km

3 ALGORITHM DESCRIPTION

This section provides a complete description of the algorithm, including both theoretical basis and technical details.

3.1 Algorithm Overview

Traditionally, estimating surface albedo from satellite multispectral TOA observations involves three steps (Liang 2004; Schaaf et al. 2008): (1) atmospheric correction; (2) surface directional reflectance modeling; (3) narrowband-to-broadband conversion. The typical example is the MODIS surface albedo algorithm. The first step corrects TOA reflectance to surface reflectance. The second step converts surface spectral reflectance into spectral albedos using kernel-driven models for individual ABI bands. Finally, the last step aggregates spectral albedos into a broadband albedo.

Instead, we propose an optimization method like the earlier algorithm used on the Meteosat data (Pinty et al. 2000a, b) to directly retrieve surface BRDF parameters, and then use the derived BRDF parameters to calculate LSA. The BRF under clear-sky conditions is estimated from atmospheric correction, while the BRF under cloudy sky conditions could be simulated from BRDF. A similar strategy was also used to retrieve daily aerosol and surface reflectance simultaneously from the Spinning Enhanced Visible and Infrared Imager (SEVIRI) on the Meteosat Second Generation (MSG) (Govaerts et al. 2010; Wagner et al. 2010). Our proposed algorithm combines atmospheric correction and surface BRDF modeling into a single optimization code (He et al. 2012). This process estimates BRDF parameters by minimizing a cost function that incorporates both TOA reflectance and albedo climatology. Our method offers several advancements over previous methods:

- Temporal Variation of AOD (Aerosol Optical Depth): We account for the temporal variability of AOD.
- Joint Optimization of Multiple Channels: Our method performs joint optimization across multiple ABI spectral channels, enabling accurate retrieval of shortwave broadband albedo.
- Alternative Radiative Transfer Formulation: We employ a different formulation for atmospheric radiative transfer.
- Incorporation of Climatological Constraints: We use both albedo and BRDF climatology as constraints within the optimization process.

Our optimization method requires the accumulation of multi-angle clear-sky observations from varying solar zenith angles. These observations can be collected over the current or previous days, assuming relatively stable surface conditions. However, continuous cloud cover may impede the accumulation of clear-sky observations and render the routine LSA algorithm inapplicable. To address these infrequent situations, we propose a backup strategy: a direct estimation approach or the use of fill values derived from albedo climatology.

3.2 Processing Outline

3.2.1 Routine processing outline

Retrieving BRDF parameters requires observations from various viewing and illumination geometries. Since the ABI sensor is not multi-angular, we achieve this by utilizing observations from different times of the day with variation in the solar zenith angle domain for each pixel. The multi-time observation database is updated daily, ideally based on clear-sky observations throughout the day. However, due to cloud cover and limited viewing angles, the algorithm may accept the nearest available TOA reflectance data within the past 14 days. This assumes that BRDF parameters exhibit relative stability over a two-week period.

To optimize code performance, our algorithm is divided into two stages: offline and online mode. The offline mode, running at the end of each day, performs a complete inversion of BRDF parameters using the accumulated hourly time series data. These calculated BRDF parameters are then stored for the next day's online mode (ideally). For increased product reliability and continuity, the online LSA algorithm can utilize BRDF parameters retrieved within the past week. If the primary algorithm based on successful BRDF retrieval fails, a backup approach called "direct estimation" is triggered within the online mode. This backup directly calculates broadband albedo from clear-sky TOA reflectance data. Alternatively, pre-computed albedo climatology is used to derive full-disk LSA products.

LSA and BRDF products are generated at various frequencies and resolutions: Every 10 minutes for full Earth disk (FD) at 2 km resolution. Every 5 minutes for the Continental United States (CONUS) region at 2 km resolution. Twice per day for 2 additional "Meso" domains (resolution not specified). The processing workflows for offline and online LSA modes are illustrated in Figures 3.1 and 3.2, respectively.

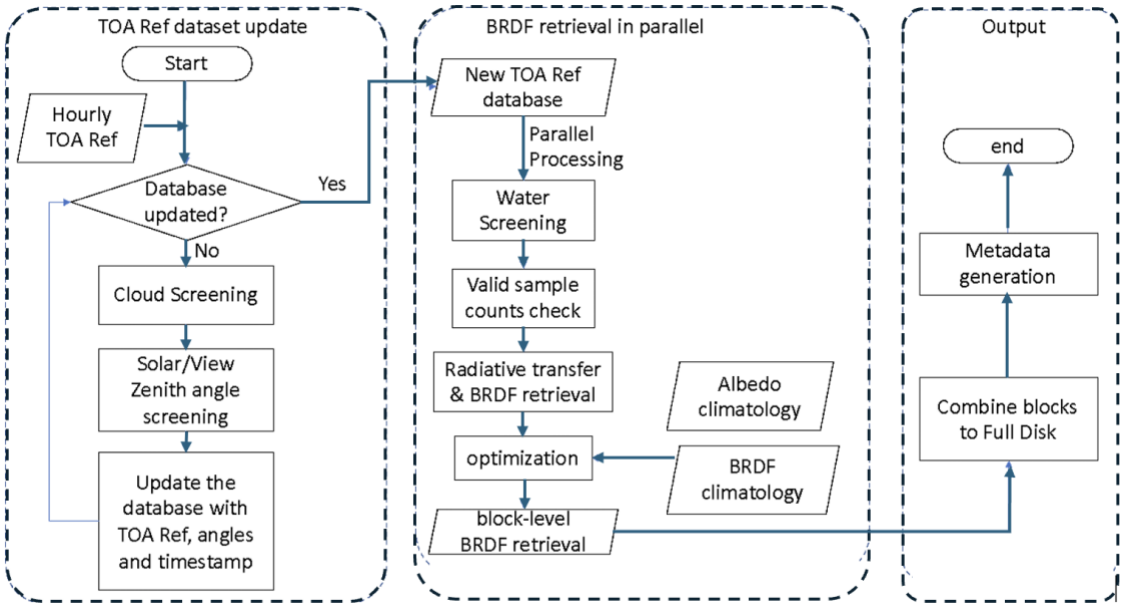

Figure 3.1. High level flowchart of the offline mode of ABI LSA algorithm, which is executed once at the end of each day to estimate the BRDF parameters.

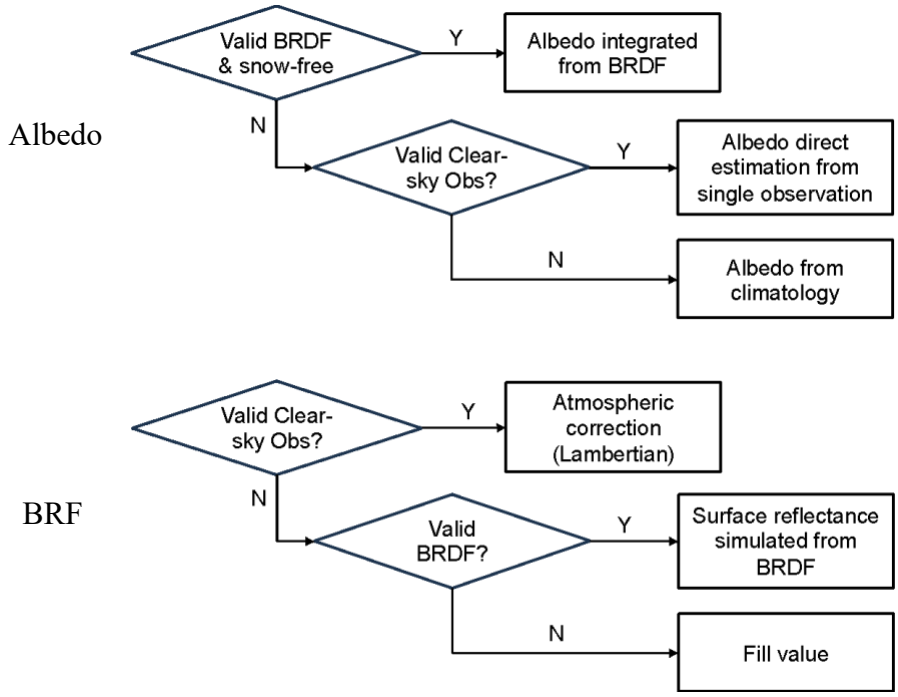

Figure 3.2. High level flowchart of the online mode of ABI LSA algorithm, illustrating the main processing components.

The LSA online algorithm uses the ABI AOD product as input when valid for accurate LSA estimation. If the ABI AOD product is unavailable, the missing AOD information will be filled with an alternative source (or method).

3.2.2 **Startup setup and interruption control**

Automatic control handling strategy needs to be designed in case of systematic exceptions. For instance, the offline algorithm relies on an accumulation of clear-sky TOA observations to composite the BRDF. The timeliness of the TOA reflectance will influence the BRDF accuracy, so is necessary to consider how to deal with TOA data missing or system interruptions. Besides, the BRDF optimization algorithm needs reliable initial value input to improve the efficiency and effectiveness. When the BRDF from the climatology is available, it can provide the initial value for the optimization. Otherwise, the algorithm will switch to an experienced initial value and broader searching range to achieve the globally optimized coefficients. The applied exception handling strategy is introduced in this section, which also guides the setup method for a startup status of the NRT operation.

1) Data availability oriented branches
   The online albedo/Reflectance retrieval requires the offline produced BRDF as input. The BRDF retrieval relies on an accumulation of TOA reflectance within a composition period. Normally, one days' FD observations have enough angle

diversity to drive the BRDF retrieval in most seasons. However, due to the cloud contamination and the geometry angle restriction, many pixels are still lack of sufficient reflectance observations after one day. Then the latest available clear-sky TOA reflectance work as a substitute. However, the time gap cannot be longer than 14 days so that the assumption of BRDF stability remains valid.

Thus, each set-up process start with an accumulation of database for 10 days to make sure clear-sky TOA reflectance dataset available for most pixels. Before the completion of this spin-up period, the BRDF retrieval sub-module will not be executed (Figure 3.3).

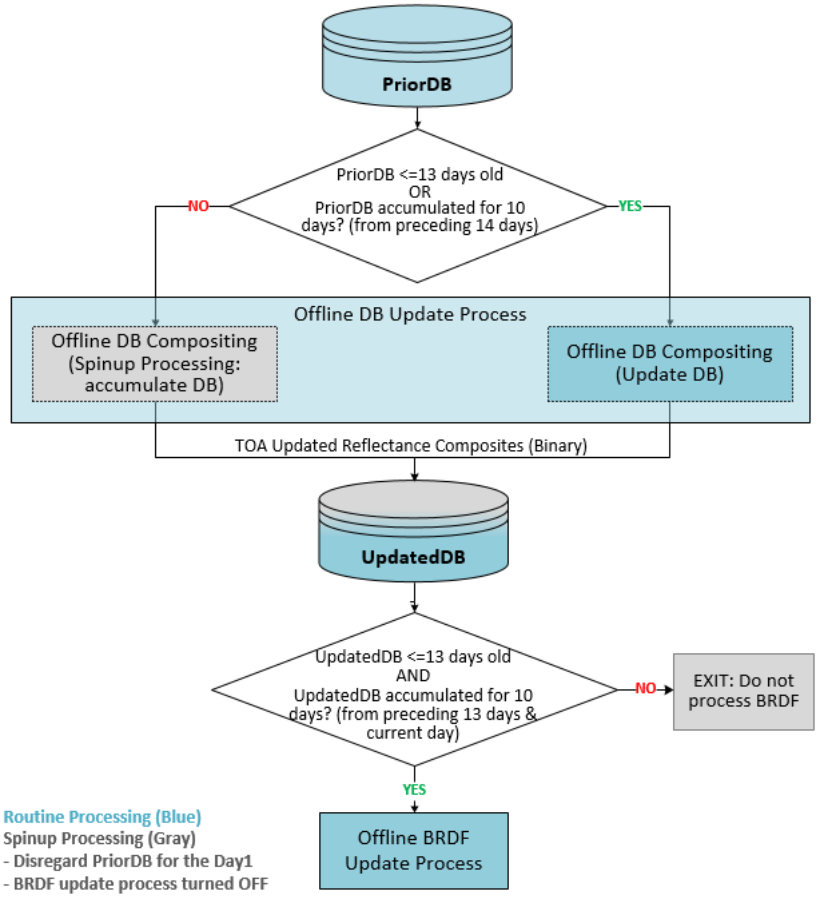

Figure 3.3 Daily calling procedure of offline procedures (DB refers to 'Database')

2) Seed data handling strategy

The offline algorithm deploys an optimization process to estimate the BRDF parameters. The BRDF climatology acts as an initial value in the optimization process accompanying and supplies the searching range in the response surface of the objective function, which will help accelerate the convergence. Otherwise, if the BRDF climatology is not available, the algorithm uses an experienced initial value and a wider searching range in the response surface. The initial values and searching range of BRDF coefficients are listed in Table 3.2. The AOD uses a fixed initial value 0.1 and a search range of [0.01, 0.24].

Table 3.1 The optimization parameter setting about coefficients.

	f_{iso}		f_{vol}		f_{geo}	
	initial	range	initial	range	initial	Range
with BRDF climatology	$f_{iso\text{-}clm\text{-}mean}$	[$f_{iso\text{-}clm\text{-}min}$, $f_{iso\text{-}clm\text{-}max$]	$f_{vol\text{-}clm\text{-}mean}$	[$f_{vol\text{-}clm\text{-}min}$, $f_{vol\text{-}clm\text{-}max$]	$f_{geo\text{-}clm\text{-}mean}$	[$f_{geo\text{-}clm\text{-}min}$, $f_{geo\text{-}clm\text{-}max$]
without previous BRDF	0.2	[0,1]	0.1	[0,0.4]	0.05	[0,0.1]

3.3 Algorithm Input

This section describes the input required to execute the LSA algorithm. The offline mode and online mode have different requirements. Tables 3.2 and 3.3 list them respectively. The input data selection criteria for offline dataset update include:

- Ten hourly observations are required for each day's database update.
- Missing data at the exact hour is acceptable if a substitute exists within a 30-minute window (15 minutes before or after the desired hour). This substitution is only valid if all other input data for that time step are also available.
- For each hourly time step, a complete set of dynamic input data is required, including L1B bands, navigation data, and cloud mask. Observations with any missing data file should be excluded from the update.

Table 3.2. Summary of inputs for ABI LSA algorithm offline mode.

Sensor input (One day's data)		TOA reflectance at five bands
		View zenith angle
		Solar zenith angle
		View azimuth angle
		Solar azimuth angle
		Navigation (Geolocation, water mask)
Ancillary data	**ABI products (One day's data)**	Cloud mask
	Non-ABI static data	Surface albedo climatology
		BRDF climatology
	Intermediate dynamic data	Clear-sky Observation Database
		Configuration file

Table 3.3 Summary of inputs for ABI LSA algorithm online mode.

Sensor input (Current timestamp)		TOA reflectance at five bands
		View zenith angle
		Solar zenith angle
		View azimuth angle
		Solar azimuth angle
		Navigation (Geolocation, Water mask)
Ancillary data	**ABI products (Current timestamp)**	Aerosol optical depth
		Cloud mask
	Non-ABI static data	Surface albedo climatology
		Atmosphere LUT
		Coefficients of direct estimation for albedo
	Intermediate dynamic data	Pre-calculated BRDF parameters
		IMS snow mask
		Configuration file

Essentially, the offline mode algorithm requires time series data for all types of input, whereas the online mode only uses datasets closest to the current observation hour, as it runs once an hour.
Additionally, the online mode requires pre-calculated BRDF parameters from offline output as input.
For a specific dataset, both the online and offline modes share the same details, which are outlined in the following subsections.

3.3.1 Primary Sensor Data

Primary sensor data consists of information derived solely from ABI observations. This data, utilized by the LSA algorithm, includes TOA reflectance values and relevant ancillary information such as angles, geolocation, and land/water masks. The spatial resolution of both LSA and BRF products is 2km, therefore, input ABI sensor data should also be aggregated to 2km.
The L1B reflectance sensor quality check (criteria found in Table 5.1.3.6.3 and Table 5.1.3.6.4 of the GOES R SERIES PUG vol3) utilizes the 4-level DQF layer in ABI L1B data along with the TOA reflectance value. If the DQF equals 0 (good_pixel_qf) and the reflectance value is within [0,1], the pixel quality is considered good. Otherwise, it is categorized as a bad pixel.

Table 3.4. Input list of primary sensor data.

Name	Type	Description	Dimension
Ch1	input	Calibrated ABI level 1b reflectance at channel 1	grid (xsize, ysize)
Ch2	input	Calibrated ABI level 1b reflectance at channel 2	grid (xsize, ysize)
Ch3	input	Calibrated ABI level 1b reflectance at channel 3	grid (xsize, ysize)

Ch5	input	Calibrated ABI level 1b reflectance at channel 5	grid (xsize, ysize)
Ch6	input	Calibrated ABI level 1b reflectance at channel 6	grid (xsize, ysize)
Latitude	input	Pixel latitude	grid (xsize, ysize)
Longitude	input	Pixel longitude	grid (xsize, ysize)
Solar zenith	input	ABI solar zenith angles	grid (xsize, ysize)
Solar azimuth	input	ABI solar azimuth angles	grid (xsize, ysize)
View zenith	input	ABI view zenith angle	grid (xsize, ysize)
View azimuth	input	ABI view azimuth angle	grid (xsize, ysize)
Land/water mask	input	ABI land/water mask	grid (xsize,ysize)

3.3.2 **Derived Sensor Data**

The LSA algorithm requires two ABI-derived sensor data products: 1) the ABI Cloud Mask (ACM) product, which classifies each pixel into one of four cloudiness states: clear, probably clear, probably cloudy, and cloudy; and 2) the ABI Aerosol Optical Depth (AOD) along with its quality flag.
The algorithm employs distinct retrieval strategies for clear-sky and cloudy conditions, as determined by the cloud mask input. Pixels with a cloud mask of 0 (Absolutely clear) and 1 (Probably clear) are processed using the clear-sky subroutine.

Table 3.5. Input list of derived sensor data.

Name	Type	Description	Dimension
Cloud mask	input	ABI cloud mask product	grid (xsize, ysize)
AOD	input	ABI AOD product	grid (xsize, ysize)

3.3.3 **Ancillary Data**

Ancillary data are data other than the ABI sensor and derived data (Table 3.6). The following list describes the ancillary data required to run the LSA algorithm. The specific types of ancillary data required are:

- **IMS snow mask data**
  This data is used to determine snow cover for each pixel.
- **LSA Climatology**
  The albedo climatology includes the mean and variance of land surface spectral and broadband albedos. This climatology provides background values for albedo estimation. Multiple years of MODIS albedo products are averaged to create the climatology, which is calculated at 8-day intervals.
- **BRDF Climatology**
  The BRDF climatology provides prior knowledge about the mean, maximum, minimum, and standard deviation of each BRDF parameter for a specific day of the

year. This climatology supplies the initial guess and search range for BRDF coefficients used in the optimization algorithm.

- **Atmospheric parameter Look-Up table**
  To improve the computational efficiency, the atmospheric parameters are pre-calculated using the Modtran simulation and stored in a look-up table (LUT). LUT is a type of static input to the algorithm and all codes share the same LUT. The parameters stored in the LUT include:
  - Atmospheric path reflectance
  - Gaseous transmittance
  - Downward scattering transmittance
  - Upward scattering transmittance
  - Total spherical albedo
  - Total optical depth
  - Direct irradiance ratio

  The entries in the LUT were selected after a sensitivity analysis to balance accuracy and computational efficiency (Table 3.7).

- **BRDF model parameters**
  BRDF model parameters are used for albedo integration. These parameters are the output of the offline mode code and the input of the online mode code.

- **Coefficients (LUTs) of direct estimation approach**
  Two groups of coefficients are stored in a look-up table (LUT) to calculate black-sky and white-sky albedo from TOA spectral reflectance, respectively. Each observing geometry has its own set of coefficients. Table 3.8 describes the LUT in more detail.

Table 3.6 Input of ancillary data.

Name	Type	Description	Dimension
Land/water mask	Input	A land-water mask	grid (xsize, ysize)
Albedo climatology	Input	Historical mean 8-day albedo	grid (xsize, ysize), 46 granules
BRDF climatology	Input	Historical mean, maximum, minimum, and standard deviation of each BRDF parameter	grid (xsize, ysize), 5*3*4 variables in a granual, 366 granules
Atmosphere LUT	Input	Five atmospheric parameters as function of aerosol optical depth, ABI channel and observing geometry	(16x 16 x 7 x 10 x 5) *
Coefficient of direct estimation approach	Input	Two groups of coefficients for calculating black-sky and white-sky albedo respectively for each observing geometry	(16x 16 x 7 x 6 x 2)
BRDF parameters	Input	BRDF_Parameters_Band1, [f_iso, f_vol, f_geo], representing the coefficient of isotropic kernel,	grid (3, xsize, ysize)

		volumetric kernel, and geometric kernel respectively	
		BRDF_Parameters_Band2, [f_iso, f_vol, f_geo],	grid (3, xsize, ysize)
		BRDF_Parameters_Band3, [f_iso, f_vol, f_geo],	grid (3, xsize, ysize)
		BRDF_Parameters_Band5, [f_iso, f_vol, f_geo],	grid (3, xsize, ysize)
		BRDF_Parameters_Band6, [f_iso, f_vol, f_geo],	grid (3, xsize, ysize)

* The LUT dimension corresponds to num_solar_zenith_angle * num_sensor_senith_angle * num_relative_azimuth_angle * num_aerosol_optical_depth * num_bands

Table 3.7 Entries of Atmospheric parameters LUT.

Entries to LUT	Values
Solar Zenith Angle	0.,5.,10.,15.,20.,25.,30.,35.,40.,45.,50.,55.,60.,65.,70.,75.
Sensor Zenith Angle	0.,5.,10.,15.,20.,25.,30.,35.,40.,45.,50.,55.,60.,65.,70.,75.
Relative Azimuth Angle	0., 30., 60., 90., 120., 150., 180.
Aerosol Optical Depth	.01,.05,.1,.15,.2,.3,.4,.6,.8,1.
Band	1,2,3,5,6

* The size of atmospheric LUT is (7, 16, 16, 7, 10, 5), corresponding to parameter, SZA, VZA, RAA, AOD, Band.

Table 3.8 Entries of Albedo (BSA/WSA) LUTs.

Entries to LUT	Values
Solar Zenith Angle	0.,5.,10.,15.,20.,25.,30.,35.,40.,45.,50.,55.,60.,65.,70.,75.
Sensor Zenith Angle	0.,5.,10.,15.,20.,25.,30.,35.,40.,45.,50.,55.,60.,65.,70.,75.
Relative Azimuth Angle	0., 30., 60., 90., 120., 150., 180.

* The size of BSA/WSA LUTs are (16, 16, 7, 5+1). The last dimension corresponds to the linear coefficients in an order of constant, coef_band1, coef_band2, coefs_band3, coefs_band5, coefs_band6.

- **Clear-sky observation database**

  The database includes both inputs and outputs of the offline mode calculations. At the end of each day, the offline code examines all the new observations and updates the database. This maintenance procedure in the offline mode mainly conducts the following steps iterating over each pixel for each timestamp:

  The database stores clear-sky observations for each hourly interval during the day (10 in total, 12~21 UTC for GOES-east location, 14~23 UTC for GOES-west location), using the observation closest to each exact hour to build the database. The clear-sky observation for each time step is collected from the day closest to the current day. Both the timestamp and solar angular information are also stored in the database. This database is updated daily by incorporating the latest clear-sky observations with their timestamps and solar angular information (Table 3.9). This

maintenance procedure in the offline mode involves iterating over each pixel for each timestamp, performing the following steps:

1) read in the reflectance database and set the time step T_i to the beginning of the day (T_0).
2) read in the TOA reflectance data the corresponding cloud mask at time step T_i.
3) check the observing geometries: if the sensor zenith is larger than 70° or the solar zenith is larger than 67°, the old data in the database will be kept go to Step 2) for the next time stamp T_{i+1}; otherwise continue with Step 4) for time step T_i.
4) check if the pixel is cloud contaminated (cloud present or cloud shadow present) according to the cloud mask and other constraints on spectral reflectance: if yes, the old data in the database will be kept and go to Step 2) for the next time stamp T_{i+1}; otherwise continue with Step 5) for time step T_i.
5) check if the L1B observations have good quality (criterion refer to Table 5.1.3.6.3 and Table 5.1.3.6.4 in GOES R SERIES PUG vol3) using the 4-level DQF layer in ABI L1B data and the reflectance value: if the DQF is not equal to 0 (good_pixel_qf) or the reflectance value is beyond [0 1], the old data in the database will be kept and go to Step 2) for the next time stamp T_{i+1}; otherwise continue with Step 6) for time step T_i.
6) update the database with the current TOA reflectance, together with its corresponding angles and acquisition time.
7) Continue with the next time stamp T_{i+1} from Step 2) until the end of the day.

Table 3.9 Details of Clear-sky observation database for each hourly interval

Name	Type	Description	Dimension
Ch1	input	Calibrated ABI level 1b reflectance at Ch1	grid (0, xsize, ysize)
Ch2	input	Calibrated ABI level 1b reflectance at Ch2	grid (1, xsize, ysize)
Ch3	input	Calibrated ABI level 1b reflectance at Ch3	grid (2, xsize, ysize)
Ch5	input	Calibrated ABI level 1b reflectance at Ch5	grid (3, xsize, ysize)
Ch6	input	Calibrated ABI level 1b reflectance at Ch6	grid (4, xsize, ysize)
Solar zenith	input	ABI solar zenith angles	grid (5, xsize, ysize)
Relative azimuth	input	ABI relative azimuth angles	grid (6, xsize, ysize)
Time stamp	input	Julian day of the clear-sky observation at T_i	grid (7, xsize, ysize)

3.4 Theoretical Description

3.4.1 BRDF Retrieving in the Offline Mode

The critical step in retrieving LSA and land surface BRF involves estimating the surface BRDF parameters. An optimization approach will serve as the routine algorithm to derive

BRDF parameters in the offline mode (Section 3.4.1). If fails, the BRDF would be filled from the BRDF climatology, but being marked as low-quality retrievals, and would not be used in the online mode. The pixelwise optimization procedure is time-consuming and is conducted daily in offline mode. The tasks of the offline mode primarily include: 1) maintaining a clear-sky TOA reflectance database, and 2) retrieving BRDF parameters using this database.

3.4.1.1 Land Surface BRDF Model

To obtain BRDF parameters, we need to execute the atmospheric correction and BRDF modeling. We achieve this in one step by combining both the atmospheric radiative transfer process and BRDF modeling in an optimization schema. Three groups of equations are introduced here: the BRDF model, the Atmospheric radiative transfer equations, and equations calculating albedo from BRDF parameters.

Performance of albedo retrieval from satellite observations is usually restricted by a limited sampling of directional surface reflectance. Therefore, a model is usually used to characterize the surface anisotropy. The model can be inverted with a finite set of angular samples and used to calculate surface reflectance in any sun-view geometry and to derive surface albedo. An empirical kernel-based BRDF model will be used in the ABI LSA algorithm.

Maignan et al. (2004) found that among the current BRDF models, the best two are the three-parameter linear Ross–Li model and the nonlinear Rahman–Pinty–Verstraete model. However, all models fail to accurately reproduce the sharp reflectance increase close to the backscattering (hotspot peak) direction. Based on physical considerations, Maignan et al. (2004) suggested a modification of the Ross–Li model, without the addition of a free parameter, to account for the complex radiative transfer within the land surfaces that leads to the hot spot signature. They illustrated that the modified linear model performs better than all others. The modified three-parameter linear Ross–Li BRDF model can be written as (Maignan et al. 2004):

$$r_{dd}(\theta_s,\theta_v,\phi) = f_{iso} + f_{vol}\cdot K_{vol}(\theta_s,\theta_v,\phi) + f_{geo}\cdot K_{geo}(\theta_s,\theta_v,\phi) \tag{1}$$

where the volumetric and geometrical kernel function has the following form:

$$K_{vol} = \frac{(\pi/2-\xi)\cos\xi + \sin\xi}{\cos\theta_s + \cos\theta_v}\left(1+\frac{1}{1+\xi/\xi_0}\right) - \frac{\pi}{4} \tag{2}$$

$$K_{geo} = O(\theta_s,\theta_v,\phi) - \sec\theta_s - \sec\theta_v + 0.5(1+\cos\xi)\sec\theta_s\sec\theta_v \tag{3}$$

and where

$$O = (t - \sin t\cos t)(\sec\theta_s + \sec\theta_v)/\pi \tag{4}$$

$$\cos t = \frac{h\sqrt{D^2 + (\tan\theta_s\tan\theta_v\sin\phi)^2}}{b(\sec\theta_s + \sec\theta_v)} \tag{5}$$

$$D = \sqrt{\tan^2\theta_s + \tan^2\theta_v - 2\tan\theta_s\tan\theta_v\cos\phi} \tag{6}$$

$$\cos\xi = \cos\theta_s \cos\theta_v + \sin\theta_s \sin\theta_v \cos\phi \tag{7}$$

and where ξ_0=0.026, $\frac{h}{b}$ =2.0, and all the angles have the unit of radian.

3.4.1.2 TOA Reflectance Formulation from BRDF

To retrieve AOD and BRDF parameters from TOA reflectance, we have to establish TOA reflectance as a function of BRDF parameters and AOD. Here, we use the formulation proposed by Qin et al. (2001). The formula for TOA reflectance $\rho(\Omega_s, \Omega_v)$ is expressed as:

$$\rho(\Omega_s, \Omega_v) = \rho_0(\Omega_s, \Omega_v) + \frac{T(\Omega_s)R(\Omega_s, \Omega_v)T(\Omega_v) - t_{dd}(\Omega_s)t_{dd}(\Omega_v)\left|R(\Omega_s, \Omega_v)\right|\bar{\rho}}{1 - r_{hh}\bar{\rho}} \tag{8}$$

where $\Omega_s \in (-\mu_s, \phi_s)$ is the solar incoming direction, and $\Omega_v \in (\mu_v, \phi_v)$ for the viewing direction. There are two groups of coefficients in the above expression that are independent of each other: atmosphere-dependent and surface-dependent. These coefficients in each group represent the inherent properties of either the atmosphere or the surface. This means that we can determine these two groups of coefficients separately.

For the atmosphere, $\rho_0(\Omega_s, \Omega_v)$ is the atmospheric reflectance associated with path radiance (zero surface reflectance), and $\bar{\rho}$ is the atmospheric spherical albedo as defined before. The transmittance matrices are defined as:

$$T(\Omega_s) = \left[t_{dd}(\Omega_s) \quad t_{dh}(\Omega_s)\right] \tag{9}$$

$$T(\Omega_v) = \left[t_{dd}(\Omega_v) \quad t_{hd}(\Omega_v)\right]^T \tag{10}$$

where the subscript T stands for transpose, each transmittance has two subscript symbols: d (directional) and h (hemispherical).

The direct transmittance (t_{dd}) has the simple analytical expression: $t_{dd}(\mu) = \exp(-\tau_t / \mu)$.

The directional-hemispheric transmittance (t_{dh}) defines the fraction of downward diffuse flux generated by atmospheric scattering as the direct beam passes through the atmosphere. It can be calculated as the ratio of the integrated sky radiance at the surface level $L^{\downarrow}(\Omega_s, \Omega_v)$ over the downward hemisphere to the TOA incoming solar radiation:

$$t_{dh}(\Omega_s) = \frac{\int_{2\pi^-} L^{\downarrow}(\Omega_s, \Omega_v)\mu_v d\Omega_v}{\mu_s F_0} \tag{11}$$

The hemispheric-directional transmittance (t_{hd}) is defined as the ratio of the integrated upwelling TOA radiance over the upper hemisphere to the upwelling flux at the surface level $F^{\uparrow}$:

$$t_{hd}(\Omega_v) = \frac{\int_{2\pi^+} L^{\uparrow}(\Omega_s, \Omega_v)\mu_s d\Omega_s}{F^{\uparrow}} \tag{12}$$

where both t_{dh} and t_{hd} have to be calculated numerically. A practical solution is to create look-up tables in advance.

For the surface, the reflectance matrix is defined as:

$$R(\Omega_s, \Omega_v) = \begin{bmatrix} r_{dd}(\Omega_s, \Omega_v) & r_{dh}(\Omega_s) \\ r_{hd}(\Omega_v) & r_{hh} \end{bmatrix} \tag{13}$$

where $r_{dd}(\Omega_s, \Omega_v)$ is the surface BRF. The directional-hemispherical reflectance $r_{dh}(\Omega_s)$ (or black-sky albedo) is defined as:

$$r_{dh}(\Omega_s) = \frac{1}{\pi}\int_{2\pi^+} r_{dd}(\Omega_s, \Omega_v) d\Omega_v \,, \tag{14}$$

where the integration is over the upper hemisphere. The hemispherical-directional reflectance $r_{hd}(\Omega_v)$ is defined in the same way, but the integration is over the lower hemisphere:

$$r_{hd}(\Omega_v) = \frac{1}{\pi}\int_{2\pi^-} r_{dd}(\Omega_s, \Omega_v) d\Omega_s \tag{15}$$

The bi-hemispherical reflectance (r_{hh})(or white-sky albedo) is:

$$r_{hh} = 2\int_0^1 r_{dh}(\mu_s)\mu_s d\mu_s \tag{16}$$

where $\mu_s = \cos(\theta_s)$.

The determinant $|R|$ is easily calculated as:

$$|R(\Omega_s, \Omega_v)| = r_{dd}(\Omega_s, \Omega_v) r_{hh} - r_{dh}(\Omega_s) r_{hd}(\Omega_v) \tag{17}$$

It is evident that if surface BRDF parameters are known, the surface reflectance matrix can be determined. The authors claim that this approach does not introduce any approximation into the formulation, and their numerical experiments demonstrate that this formulation is very accurate (Qin et al., 2001).

3.4.1.3 Calculation of Albedos from BRDF

After obtaining BRDF parameters, it is straightforward to calculate spectral black-sky albedo, which are simply integrations of the surface directional reflectance functions over the entire viewing hemisphere. The spectral albedos are denoted as narrowband albedos in the next section. Instead of directly carrying out the numeric integration, we calculate the integral using an empirical polynomial equation of the three kernel parameters, similar to

the MODIS albedo algorithm (Schaaf et al. 2002), fitting black-sky albedo with a polynomial function:

$$\alpha_{bs}(\theta_s) = f_{iso}a + f_{vol}(b_0 + b_1\theta_s + b_2\theta_s^2 + b_3\theta_s^3 + b_4\theta_s^4 + b_5\theta_s^5) + f_{geo}(c_0 + c_1\theta_s + c_2\theta_s^2 + c_3\theta_s^3 + c_4\theta_s^4 + c_5\theta_s^5) \quad (18)$$

Where θ_s is the solar zenith angle, and $a, b_0, b_1, b_2, b_3, b_4, b_5, c_0, c_1, c_2, c_3, c_4, c_5$ are the regression coefficients, whose values are listed in Table 3.10. Similarly, the white-sky albedo can be computed by using the equation:

$$\alpha_{ws} = f_{iso}a + f_{vol}b + f_{geo}c \quad (19)$$

Table 3.9. Coefficients used to calculate albedo from BRDF parameters.

Variable	Value	Variable	Value
a	1.0	c_0	-1.2661
b_0	-0.0003	c_1	-0.4434
b_1	0.3368	c_2	2.2809
b_2	-1.7243	c_3	-4.8262
b_3	4.01077	c_4	3.9824
b_4	-3.4934	c_5	-1.1456
b_5	1.1442		
a	1.0		
b	0.2260		
c	-1.3763		

After the narrowband albedos are obtained from the integration of the directional reflectance model, narrowband to broadband conversions are carried out based on empirical statistical relationships. The broadband albedo mainly depends on surface spectral albedo spectra but is also affected by the atmospheric conditions. With extensive radiative transfer simulations and surface reflectance spectral measurements, we have developed the conversion formulas for calculating the total shortwave albedo, total-, direct-, and diffuse-, visible, and near-infrared broadband albedos for several narrowband sensors (Liang 2001; Liang et al. 2003; Liang et al. 1999), including ASTER, AVHRR, GOES, Landsat-7 ETM+, MISR, MODIS, POLDER, and VEGETATION in SPOT spacecraft. A similar approach was later applied to generate the conversion formula for VIIRS (Liang et al. 2005a). The formula for MODIS has been used for routine albedo production (Schaaf et al. 2002), the MISR formula for calculating shortwave albedo is very effective (Chen et al. 2008), and the VIIRS formula will be used for operational albedo production. The same strategy also will be used to covert five ABI narrowband albedos to one broadband albedo. The broadband albedo can be converted from spectral albedos using the following empirical formula:

$$\bar{r}(\theta_s) = \beta_0 + \beta_1 F_1 r_1(\theta_s) + \beta_2 F_2 r_2(\theta_s) + \beta_3 F_3 r_3(\theta_s) + \beta_5 F_5 r_5(\theta_s) + \beta_6 F_6 r_6(\theta_s) \quad (20)$$

where $r_i(\theta_s)$ are the spectral albedo, β_i are the coefficients, F_i are the normalized downward irradiance of the ABI five bands:

$$F_i = \frac{E_i(\theta_s)}{E_1(\theta_s) + E_2(\theta_s) + E_3(\theta_s) + E_5(\theta_s) + E_{6i}(\theta_s)} \tag{21}$$

and are the downward irradiance of each band (at the specific solar zenith angle). Radiative transfer simulations and statistical analysis provide the coefficients β_i. The equations used for three sensors are given below:

$$\alpha_{MODIS} = 0.160\alpha_1 + 0.291\alpha_2 + 0.243\alpha_3 + 0.116\alpha_4 + 0.112\alpha_5 + 0.0713\alpha_7 - 0.0015$$

$$\alpha_{SEVIRI} = 0.4331\alpha_1 + 0.3939\alpha_2 + 0.1136\alpha_3 - 0.0084$$

$$\alpha_{ABI} = 0.2692\alpha_1 + 0.1661\alpha_2 + 0.3841\alpha_3 + 0.1138\alpha_5 + 0.0669\alpha_6$$

3.4.1.4 Derivation of BRDF Parameters using Optimization

Given the surface BRDF model (1) and the atmospheric radiative transfer model (8), the BRDF parameters and AOD at each observation can be obtained by minimizing the following cost function:

$$J(x) = (r(x) - r_b)B^{-1}(r(x) - r_b) + (\hat{\rho}(x) - \rho)R^{-1}(\hat{\rho}(x) - \rho) \tag{22}$$

where $\boldsymbol{x}$ are the three coefficients of the surface BRDF model and AOD, $r(x)$ is the calculated white-sky surface albedo using the BRDF model, r_b are the "first-guess" values of albedo from albedo climatology, B is the uncertainty matrix of the albedo "first-guess" values, ρ is the observed ABI TOA reflectance, $\hat{\rho}$ is the calculated TOA reflectance from equation (8), and R is the error matrix of the calculated TOA reflectance.

In this cost function, r_b is from the albedo climatology, B and R are preset values and adjust the relative weight of albedo and reflectance in the cost function; ρ is the observed TOA reflectance. Given one group of BRDF parameters, the white-sky surface albedo could be calculated easily (see Section 3.4.1.1.3). Given AOD in addition to BRDF parameters, the TOA spectral reflectance could be calculated from the Qin's radiative transfer equation (8) (see Section 3.4.1.1.2). In this optimization system, the parameters to be optimized are spectral BRDF parameters and AOD. There are many different approaches available to minimize the cost function and obtain the BRDF parameters. We employ the Shuffled Complex Evolution method (SCE-UA, Duan et al. (1992) and Duan et al. (1993)), an efficient algorithm in searching global optimal. The SCE-UA method is capable of handling high parameter dimensionality, and it does not rely on the availability of an explicit expression for the objective function or the derivatives.

3.4.2 Albedo Estimation Sub-routines in the Online Mode

Based on the outcomes of two tests—the successful return from offline mode and the availability of clear-sky observations within a 60-minute window—the online mode adopts different approaches to calculating albedos and BRFs. For this, clear-sky observations must be of good quality in L1B data. Cloud condition detection and sensor quality checks are conducted simultaneously.

The L1B reflectance sensor quality check (as specified in Table 5.1.3.6.3 and Table 5.1.3.6.4 of the GOES R SERIES PUG vol3) utilizes the 4-level DQF layer in ABI L1B data along with the TOA reflectance value. If the DQF equals 0 (good_pixel_qf) and the reflectance value is within the range [0,1], the pixel quality is considered good; otherwise, it is deemed a bad pixel. Cloud detection employs the ABI cloud mask. Primary algorithms are applied to each clear-sky surface pixel (categorized as "Absolutely-clear" or "Probably clear" by the 4-level cloud mask) that exhibits good sensor quality.

3.4.2.1 Albedo Routine Algorithm

If the offline mode returns successfully, the online mode uses the retrievals of BRDF parameters from the offline mode to calculate albedos. This is called the routine algorithm. Using equations (18) and (19), we can obtain both black-sky and white-sky spectral albedos. The broadband black-sky and white-sky albedos could then be derived from Equation (20).

Given the black-sky and white-sky broadband albedo, the blue-sky broadband albedo α can be calculated by:

$$\alpha = p\alpha_{ws} + (1-p)\alpha_{bs} \tag{23}$$

where p is the diffuse fraction of the total radiation. 1-p is the direct fraction of the total radiation. The fraction of direct irradiance is one parameter of the LUT. Given AOD, the corresponding p could be searched from the LUT. If no AOD value is available, the default value of 0.1 will be used in searching LUT.

3.4.2.2 Albedo back-up algorithm

The routine optimization algorithm requires the aggregation of multiple-angle clear-sky observations. In contrast, the direct estimation approach uses only one set of clear-sky observations at a time as its input. Validation demonstrates that this approach can produce reliable albedos over both "dark" and "bright" surfaces. The Joint Polar Satellite System (JPSS) VIIRS albedo product has implemented this approach as its operational algorithm (Wang et al. 2013).

The mathematical formulation of this approach is straightforward. Extensive simulations of atmospheric radiative transfer have demonstrated a strong relationship between surface albedo and TOA spectral reflectance when the observing geometry is fixed. Thus, the direct estimation approach calculates surface albedo directly from TOA signals.

For a given combination of solar zenith angle θ_s, view zenith angle θ_v and relative azimuth angle φ, surface albedo α could be calculated from TOA spectral reflectance $\rho_i(\theta_s,\theta_v,\varphi)$ at five bands (i=1,2,3,5,6) using a linear equation:

$$\alpha = a_0(\theta_s,\theta_v,\varphi) + \sum_{i=1,2,3,5,6} a_i(\theta_s,\theta_v,\varphi)\rho_i(\theta_s,\theta_v,\varphi) \tag{24}$$

where $a_i(\theta_s,\theta_v,\varphi)$ (i=0,1,2,3,5,6) are preset coefficients dependent on the viewing geometry. The regression coefficients were derived offline through extensive simulations of atmospheric radiative transfer. Two sets of coefficients are stored separately for calculating white-sky albedo and black-sky albedo.

3.4.2.3 Albedo graceful degradation estimation from climatology

If no clear-sky observations are available and no BRDF parameters have been retrieved, meaning the previous two subroutines have failed, we have to find an alternative method to predict albedo, rather than resorting to providing filler values. Yang et al. (2008) provided an empirical equation to calculate black-sky albedo α_{bs} from white-sky albedo α_{ws} when the solar zenith angle θ is known:

$$\alpha_{bs} = \alpha_{ws}\frac{1+1.14}{1+1.48\cos\theta} \tag{25}$$

We use this equation to predict instantaneous albedo from the climatological white-sky albedo when no clear-sky observation is available and no BRDF parameters have been retrieved.

3.4.3 BRF estimating sub-routines in the online mode

In the online mode, surface BRF products are produced every 60 minutes. ABI will obtain four sets of images within the 60-minutes window. Depending on the availability of clear-sky observation at the timestamp and BRDF parameters from the offline process, the calculation of surface BRF are led to several different paths over each pixel:
In the online mode, surface BRF products are generated every 60 minutes. ABI captures four sets of images within each 60-minute window. Depending on the availability of clear-sky observations at the timestamp and the BRDF parameters from the offline process, the calculation of surface BRF follows several different paths for each pixel:

1. When valid clear-sky observations exist:
    a. BRF is retrieved through atmospheric correction, assuming a Lambertian surface, with the latest clear-sky observation as input (algorithm R3).
2. When clear-sky observations are not valid:
    a. If BRDF coefficients from the offline process are available, BRF is simulated from these coefficients under specific illumination and viewing geometries (algorithm R2).

b. If no BRDF coefficients have been retrieved from the routine offline process, a filler value is provided.

3.4.3.1 Prediction BRF from BRDF model

BRF can always be calculated from the BRDF model (1), given the BRDF parameters and viewing geometry. Numerically, BRF is related to BRDF as follows:

$$BRF = BRDF * \pi \tag{26}$$

However, the BRDF parameters retrieved from the offline mode represent the average surface conditions over the compositing period. Significant uncertainties arise when predicting instantaneous surface BRF using these offline BRDF parameters. This prediction serves as a backup method when no clear-sky observations are available. For this subroutine, the retrieval path flag is marked as 1.

3.4.3.2 Lambertian atmospheric correction from TOA observations

This is the main sub-routine for BRF estimation, and the retrieval path flag is marked as 2. We assume the surface is Lambertian, resulting in a simplified form of equation (8):

$$r = r_0 + \frac{r_s}{1 - r_s \rho} \gamma \tag{27}$$

where r represents TOA reflectance, r_s indicates surface reflectance, ρ refers to spherical albedo, r_0 denotes path reflectance, and γ symbolizes transmittance. Given the viewing geometry and AOD, ρ, r_0 and γ could be obtained from the LUT. Thus, the surface reflectance could be determined using the following equation:

$$r_s = \frac{r - r_0}{\gamma + (r - r_0)\rho} \tag{28}$$

If the reflectance is out of range (negative, or greater than 1 for snow pixel, or greater than 0.8 for non-snow pixel), the algorithm will use BRDF estimation subroutine for reflectance.

3.5 Algorithm Output

The outputs of the LSA algorithm offline mode mainly include the three parameters of the BRDF model for each ABI band (Table 3.11), which will be used as one input of the online mode. The final outputs of the LSA algorithm online mode are instantaneous LSA and BRFs (Table 3.12 and 3.13).

Table 3.10. Outputs of the ABI albedo algorithm offline mode.

Name	Type	Description	Dimension
Ch1 f_iso	float	BRDF isotropic component parameter at Ch1	grid (xsize, ysize)
Ch1 f_vol	float	BRDF volumetric kernel parameter at Ch1	grid (xsize, ysize)
Ch1 f_geo	float	BRDF geometric kernel parameter at Ch1	grid (xsize, ysize)
Ch2 f_iso	float	BRDF isotropic component parameter at Ch2	grid (xsize, ysize)

Ch2 f_vol	float	BRDF volumetric kernel parameter at Ch2	grid (xsize, ysize)
Ch2 f_geo	float	BRDF geometric kernel parameter at Ch2	grid (xsize, ysize)
Ch3 f_iso	float	BRDF isotropic component parameter at Ch3	grid (xsize, ysize)
Ch3 f_vol	float	BRDF volumetric kernel parameter at Ch3	grid (xsize, ysize)
Ch3 f_geo	float	BRDF geometric kernel parameter at Ch3	grid (xsize, ysize)
Ch5 f_iso	float	BRDF isotropic component parameter at Ch5	grid (xsize, ysize)
Ch5 f_vol	float	BRDF volumetric kernel parameter at Ch5	grid (xsize, ysize)
Ch5 f_geo	float	BRDF geometric kernel parameter at Ch5	grid (xsize, ysize)
Ch6 f_iso	float	BRDF isotropic component parameter at Ch6	grid (xsize, ysize)
Ch6 f_vol	float	BRDF volumetric kernel parameter at Ch6	grid (xsize, ysize)
Ch6 f_geo	float	BRDF geometric kernel parameter at Ch6	grid (xsize, ysize)
QF	char	Quality flag for each pixel, indicating the general retrieval quality	grid (xsize, ysize)

Name	Type	Description	Dimension
BRDF_ Parameters_ Band1	float	BRDF isotropic component parameter at Ch1	grid (xsize, ysize)
	float	BRDF volumetric kernel parameter at Ch1	grid (xsize, ysize)
	float	BRDF geometric kernel parameter at Ch1	grid (xsize, ysize)
BRDF_ Parameters_ Band2	float	BRDF isotropic component parameter at Ch2	grid (xsize, ysize)
	float	BRDF volumetric kernel parameter at Ch2	grid (xsize, ysize)
	float	BRDF geometric kernel parameter at Ch2	grid (xsize, ysize)
BRDF_ Parameters_ Band3	float	BRDF isotropic component parameter at Ch3	grid (xsize, ysize)
	float	BRDF volumetric kernel parameter at Ch3	grid (xsize, ysize)
	float	BRDF geometric kernel parameter at Ch3	grid (xsize, ysize)
BRDF_ Parameters_ Band5	float	BRDF isotropic component parameter at Ch5	grid (xsize, ysize)
	float	BRDF volumetric kernel parameter at Ch5	grid (xsize, ysize)
	float	BRDF geometric kernel parameter at Ch5	grid (xsize, ysize)
BRDF_ Parameters_ Band6	float	BRDF isotropic component parameter at Ch6	grid (xsize, ysize)
	float	BRDF volumetric kernel parameter at Ch6	grid (xsize, ysize)
	float	BRDF geometric kernel parameter at Ch6	grid (xsize, ysize)
BRDF_QF	char	Quality flag for each pixel, indicating the general retrieval quality	grid (xsize, ysize)

Table 3.11. Outputs of the ABI albedo algorithm online mode: LSA

Name	Type	Description	Dimension
LSA	short	Shortwave broadband albedo value at 0.4-3.0 μm	grid (xsize, ysize)
DQF	ubyte	Quality flag for each pixel, indicating the general retrieval quality	grid (xsize, ysize)

Table 3.12. Outputs of the ABI albedo algorithm online mode: BRF

Name	Type	Description	Dimension
BRF1	short	Derived bidirectional reflectance value at 0.47 μm	grid (xsize, ysize)
BRF2	short	Derived bidirectional reflectance value at 0.64 μm	grid (xsize, ysize)
BRF3	short	Derived bidirectional reflectance value at 0.86 μm	grid (xsize, ysize)
BRF5	short	Derived bidirectional reflectance value at 1.61 μm	grid (xsize, ysize)
BRF6	short	Derived bidirectional reflectance value at 2.26 μm	grid (xsize, ysize)
DQF	ubyte	Quality flag for each pixel, indicating the general retrieval quality	grid (xsize, ysize)

The GOES-R ABI LSA and BRF products are generated through multiple paths, each with varying levels of uncertainty. Detailed quality information is critical for end users. Correspondingly, we have three groups of Quality Flags (QF): one for the intermediate BRDF parameter products, a second for albedo products, and a third for reflectance products. These three groups of QFs are defined in Tables 3.14-16.

Table 3.13. QF definition of ABI intermediate BRDF parameter products

Bit	Name	Value
0	Overall quality	0: BRDF successfully retrieved 1: Routine algorithm fails
1	BRDF database age	0: at least five observations within 1 day 1: at least five observations within 2 days 2: at least five observations within 3 days 3: at least five observations within 4 days 4: at least five observations within 5 days 5: at least five observations within 6 days 6: at least five observations > 6 days 7: fill value
2		
3		
4	Climatology availability	0: valid BRDF climatology 1: invalid BRDF climatology
5		
6		
7		

Table 3.14. QF definition of ABI LSA products

Bit	Name	Value
0	overall quality	0: high quality (Routine algorithm & age<=1) 1: medium quality ((Routine algorithm & age>1) or (Back-up algorithm)) 2: low quality (Graceful degradation) 3: fill
1		
2	zenith angles	0:SZA<67 & LZA<70 1: either angle beyond favorable range
3	Retrieval path	00:Routine algorithm, 01:Back-up algorithm, 10: Graceful degradation,11: No retrieval
4		
5	BRDF age	0: 1 day 1: >1 days
6	Land mask	0:land, 1: water
7	snow	0: snow-free 1: snow

Table 3.15. QF definition of ABI BRF products

Bit	Name	Value	
0	Quality score	0: Good 1: Snow 2: Heavy aerosol (AOD>0.5) 3: Fixed aerosol (AOD=0.05) 4: Cloudy (not absolutely clear) 5: large SZA 6: large VZA 7: Bad L1b	0~1: high 2~3: medium 4: low 5~7: invalid *AOD > 0.9, heavy AOD AOD>0.5, hazy
1			
2			
3	Retrieval path	00:R1, 01:R2, 10: R3,11: at least one band has no retrieval	R3 is the main subroutine for clear-sky R1 is the backup subroutine
4			
5	small scattering angle	0: scattering angle > 5 degree 1: scattering angle < 5 degree	scattering angle to catch approximate hotspot scope
6	cloud	0: absolutely clear 1: probably clear, probably cloudy, absolutely cloudy	
7	AOD availability	0: valid AOD 1: invalid climatology	

Besides the QF info, each file of BRDF parameters, LSA and BRF products also comes with metadata information. The metadata information is given in Tables 3.17-19.

Table 3.16. Attributes or Metadata of ABI intermediate BRDF parameter products

Metadata	Source	Definition
Dimensions	Common	Number of rows/ columns/ bands
FillValue	BRDF_Parameters/ BRDF_QF	"-999.f"/"-128b"
long_name	BRDF_Parameters/ BRDF_QF	"Bidirectional reflectance distribution function parameters"/ "Bidirectional reflectance distribution function quality flag" (0 is successful retrieval; 1 is unsuccessful retrieval)
units	BRDF_Parameters/ BRDF_QF	"1"/ "1" (Dimensionless)
valid_range	BRDF_Parameters/ BRDF_QF	"0.f, 1.f"/ "0b, 1b"
Conventions	Global attribute	"CF-1.5"
summary	Global attribute	"Bidirectional reflectance distribution function parameters that describes the directional properties of reflectivity"
cdm_data_type	Global attribute	"Image"
platform_id	Global attribute	"G16"
orbital_slot	Global attribute	"GOES-East"
instrument_type	Global attribute	"GOES-R Series Advanced Baseline Imager"
spatial_resolution	Global attribute	"2km at nadir"
scene_id	Global attribute	"Full Disk"

Table 3.17. Attributes or Metadata of ABI LSA products

Metadata	Source	Definition
Date	common	Beginning and end dates of the product
Time	common	Beginning and end times of the product
Dimension	common	Number of rows, number of columns
Product Name	common	The ABI land surface albedo product
Satellite	common	GOES-R satellite name
Instrument	common	ABI
Version	common	Product version number
Filling Value	LSA	Value representing no data produced
Valid Range	LSA	Valid range of albedo values, 0-1
MeanAlb	LSA[1]	Average Albedo value
StdAlb	LSA[1]	Standard deviation of Albedo
MaxAlb	LSA[1]	Maximum Albedo value
MinAlb	LSA[1]	Minimum Albedo value
AlbPercHighQuality	LSA QC2	Percentage of High Quality Retrieval
AlbPercMedQuality	LSA QC2	Percentage of medium Quality Retrieval
AlbPercLowQuality	LSA QC2	Percentage of low Quality Retrieval
AlbPercInvalid	LSA QC2	Percentage of Invalid Retrieval

AlbPercRoutineAlgorithm	LSA QC2	Percentage of pixels using routine algorithm
AlbPercBackupAlgorithm	LSA QC2	Percentage of pixels using backup algorithm
AlbPercGracefulAlgorithm	LSA QC2	Percentage of pixels using graceful algorithm
AlbPercNoRetrieval	LSA QC2	Percentage of pixels with no retrieval
AlbPercNewBRDF	LSA QC2	Percentage of pixels with BRDF within 1day
AlbPercOldBRDF	LSA QC2	Percentage of pixels with BRDF older than 1 day
AlbPercSnowFree	LSA QC2	Percentage of snow free land pixels
AlbPercSnowCovered	LSA QC2	Percentage of snow covered land pixels

Table 3.18. Attributes or Metadata of ABI BRF products

Metadata	Source	Definition
Date	common	Beginning and end dates of the product
Time	common	Beginning and end times of the product
Dimension	common	Number of rows, number of columns
Product Name	common	The ABI land surface reflectance product
Satellite	common	GOES-R satellite name
Instrument	common	ABI
Version	common	Product version number
Filling Value	BRF	Value representing no data produced
Valid Range	BRF	Valid range of reflectance values, 0-2
MaxRef1	BRF[1]	Maximum Reflectance Band1
MinRef1	BRF[1]	Minimum Reflectance Band1
MeanRef1	BRF[1]	Average Reflectance Band1
StdRef1	BRF[1]	Standard deviation of Reflectance Band 1
MaxRef2	BRF[1]	Maximum Reflectance Band2
MinRef2	BRF[1]	Minimum Reflectance Band2
MeanRef2	BRF[1]	Average Reflectance Band2
StdRef2	BRF[1]	Standard deviation of Reflectance Band 2
MaxRef3	BRF[1]	Maximum Reflectance Band3
MinRef3	BRF[1]	Minimum Reflectance Band3
MeanRef3	BRF[1]	Average Reflectance Band3
StdRef3	BRF[1]	Standard deviation of Reflectance Band 3
MaxRef5	BRF[1]	Maximum Reflectance Band5
MinRef5	BRF[1]	Minimum Reflectance Band5
MeanRef5	BRF[1]	Average Reflectance Band5
StdRef5	BRF[1]	Standard deviation of Reflectance Band 5
MaxRef6	BRF[1]	Statistics from Ch6 Ref
MinRef6	BRF[1]	Statistics from Ch6 Ref
MeanRef6	BRF[1]	Statistics from Ch6 Ref
StdRef6	BRF[1]	Statistics from Ch6_Ref
PercHighQuality	BRF QC2	Percentage of pixels with high quality
PercMedQuality	BRF QC2	Percentage of pixels with high or fixed AOD
PercLowQuality	BRF QC2	Percentage of pixels with cloud

PercPixelsInvalid	BRF QC2	Percentage of pixels with high angle or invalid SDR
PercAODvalid	BRF QC2	Percentage of pixels with valid AOD
PercAODInvalid	BRF QC2	Percentage of pixels with invalid AOD
PercAbsClear	BRF QC2	Percentage of pixels absolutely clear
PercCloudy	BRF QC2	Percentage of pixels not absolutely clear
PercSmallScatter	BRF QC2	Percentage of pixels of small scatter angle

*Note:
1. The statistics items are calculated on the pixels with valid retrievals (i.e., $0 \leq LSA \leq 1, 0 \leq BRF \leq 2$);
2. The Percents items are calculated from the on-earth-pixels, i.e, excluding the space pixels in both the numerator and the denominator. The space pixel mask is included in L1B navigation data.

4 TEST DATA SETS AND OUTPUTS

The algorithm was tested using simulation data, AHI data, and ABI data. Both LSA products and BRF products have been validated.

4.1 Sample Output

Figures 4.1 to 4.6 show sample images of online albedo and reflectance from GOES-16 (east), GOES-17 (west), and GOES-18 (west), respectively. The BRFs are demonstrated as pseudo-color images.

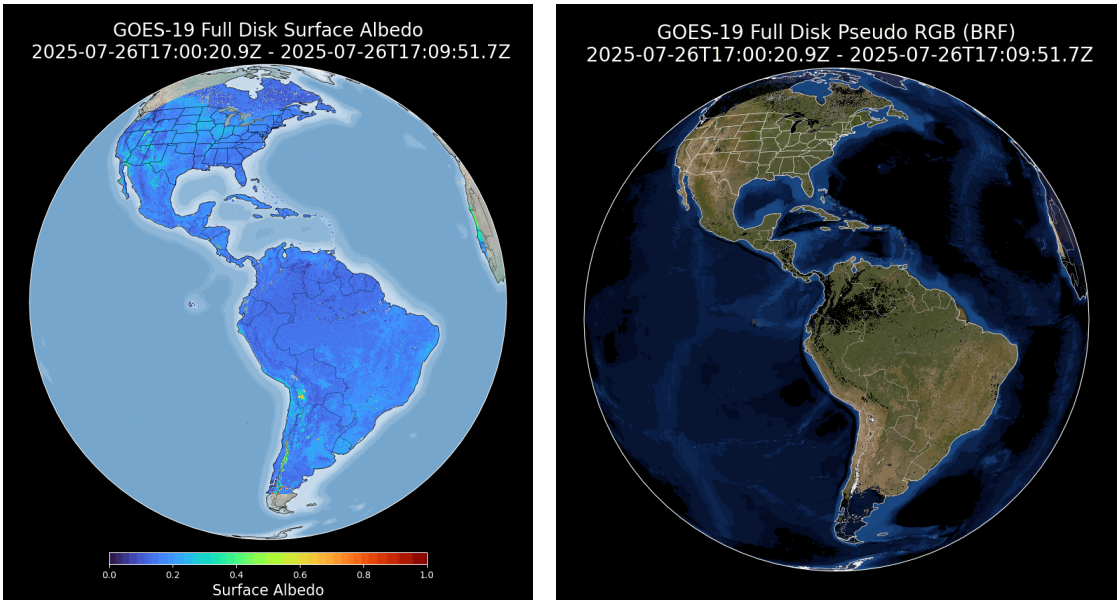

Figure 4.1 Plots of GOES-east Full Disk Albedo (left) and Pseudo-color image from BRF (right) on July 26, 2025 at 17:09 UTC.

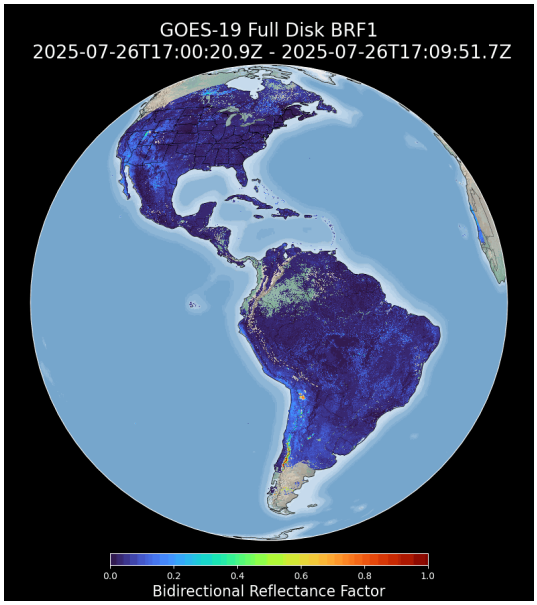
GOES-19 Full Disk BRF1
2025-07-26T17:00:20.9Z - 2025-07-26T17:09:51.7Z
0.0 0.2 0.4 0.6 0.8 1.0
Bidirectional Reflectance Factor

(a)

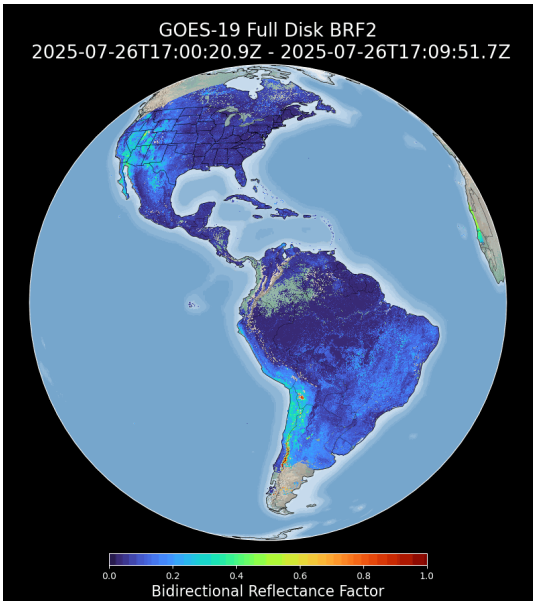
GOES-19 Full Disk BRF2
2025-07-26T17:00:20.9Z - 2025-07-26T17:09:51.7Z
0.0 0.2 0.4 0.6 0.8 1.0
Bidirectional Reflectance Factor

(b)

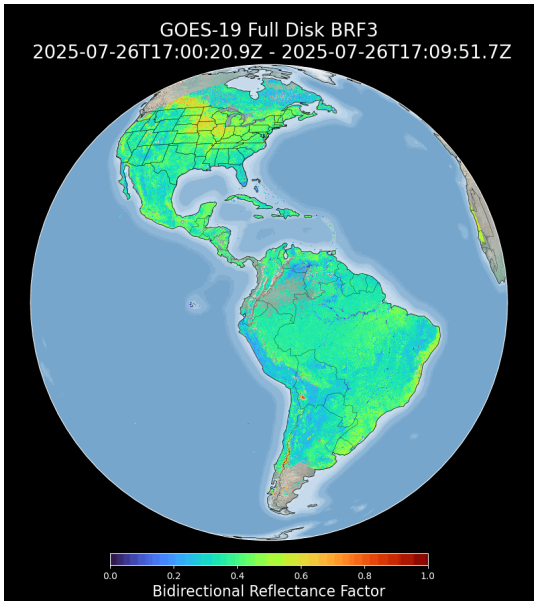
GOES-19 Full Disk BRF3
2025-07-26T17:00:20.9Z - 2025-07-26T17:09:51.7Z
0.0 0.2 0.4 0.6 0.8 1.0
Bidirectional Reflectance Factor

(c)

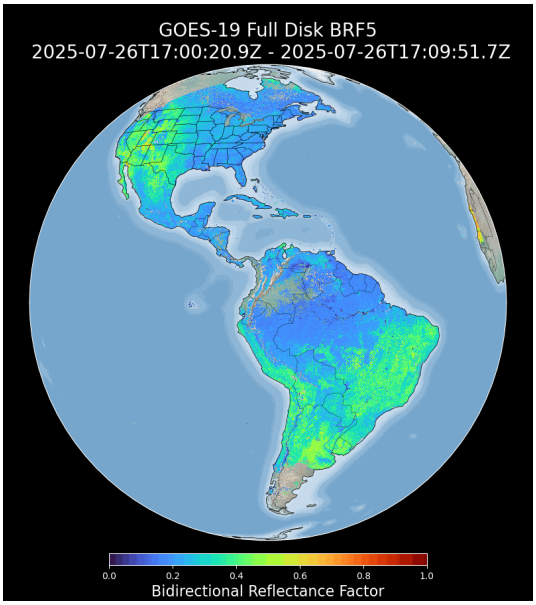
GOES-19 Full Disk BRF5
2025-07-26T17:00:20.9Z - 2025-07-26T17:09:51.7Z
0.0 0.2 0.4 0.6 0.8 1.0
Bidirectional Reflectance Factor

(d)

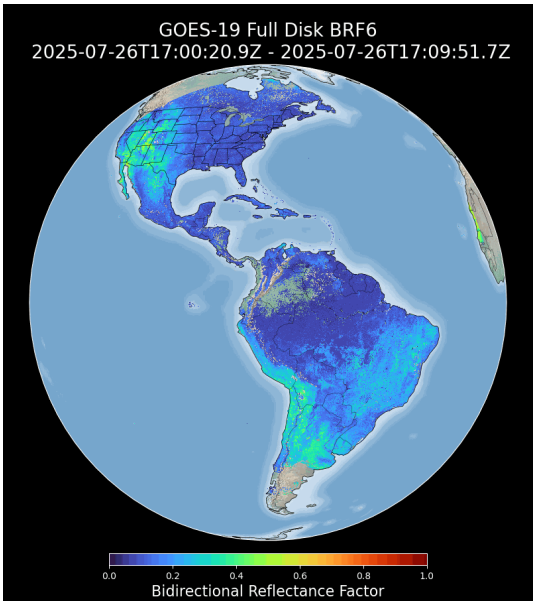

(e)

Figure 4.2 Plots of GOES-east Full Disk BRF (a) Band 1 (b) Band 2 (c) Band 3 (d) Band 5 (e) Band 6 on July 26, 2025 at 17:09 UTC.

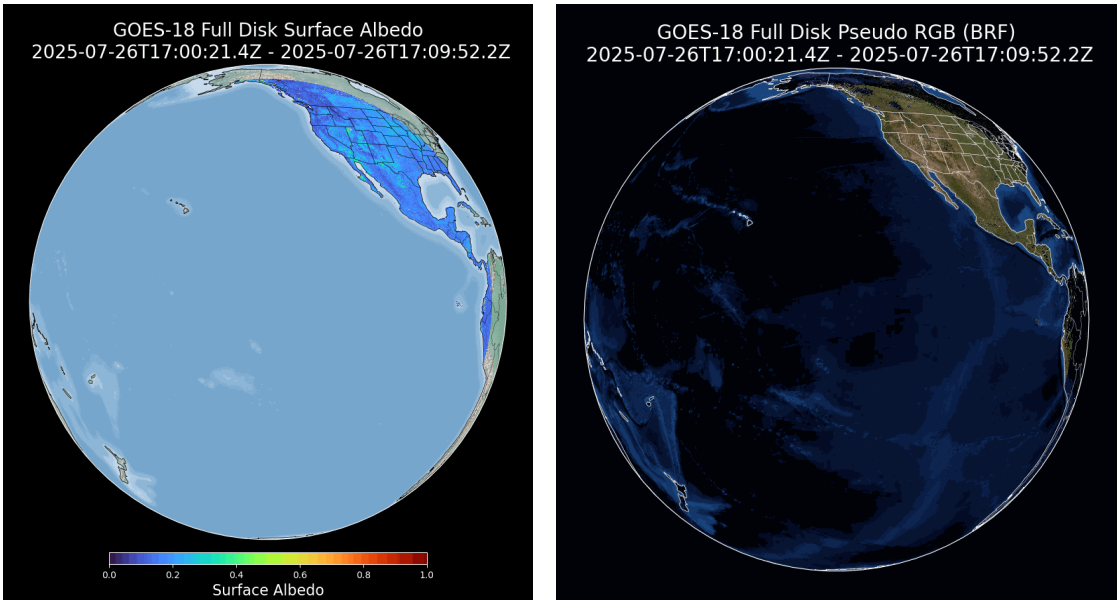

Figure 4.3 Plots of GOES-west Full Disk Albedo (left) and Pseudo-color image from BRF (right) on July 26, 2025 at 17:09 UTC.

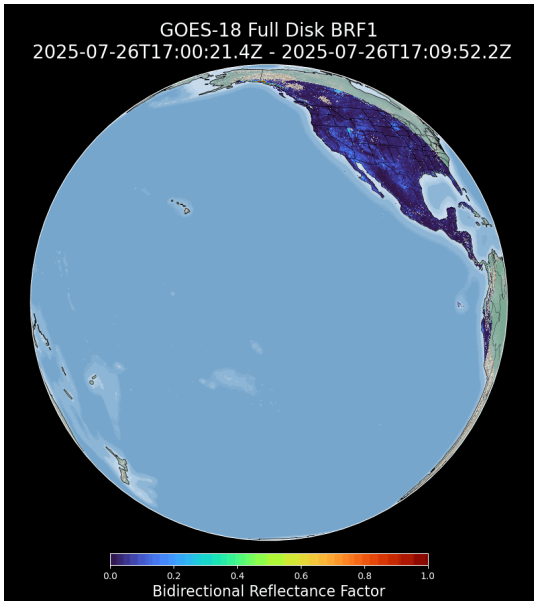
GOES-18 Full Disk BRF1
2025-07-26T17:00:21.4Z - 2025-07-26T17:09:52.2Z
0.0 0.2 0.4 0.6 0.8 1.0
Bidirectional Reflectance Factor

(a)

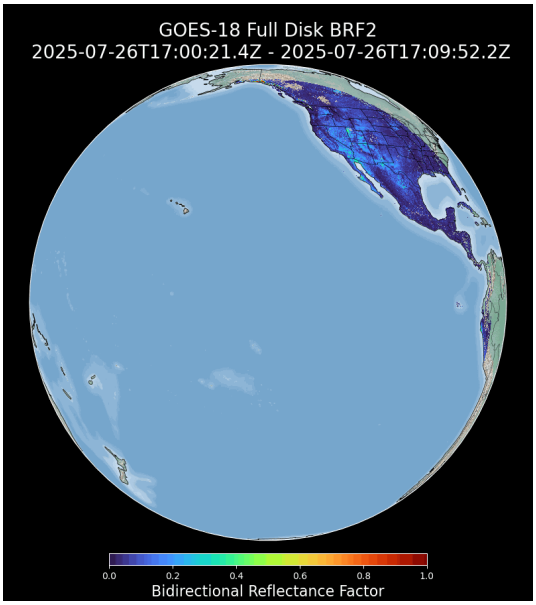
GOES-18 Full Disk BRF2
2025-07-26T17:00:21.4Z - 2025-07-26T17:09:52.2Z
0.0 0.2 0.4 0.6 0.8 1.0
Bidirectional Reflectance Factor

(b)

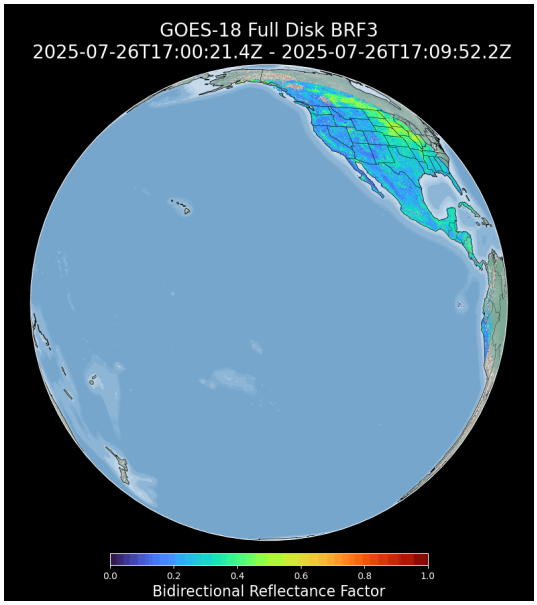
GOES-18 Full Disk BRF3
2025-07-26T17:00:21.4Z - 2025-07-26T17:09:52.2Z
0.0 0.2 0.4 0.6 0.8 1.0
Bidirectional Reflectance Factor

(c)

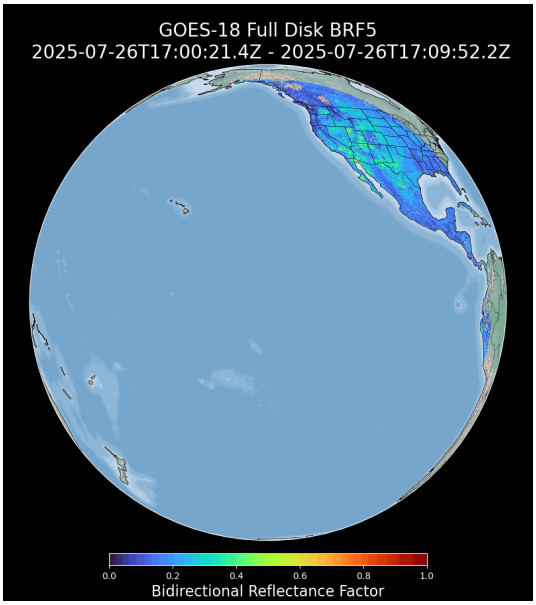
GOES-18 Full Disk BRF5
2025-07-26T17:00:21.4Z - 2025-07-26T17:09:52.2Z
0.0 0.2 0.4 0.6 0.8 1.0
Bidirectional Reflectance Factor

(d)

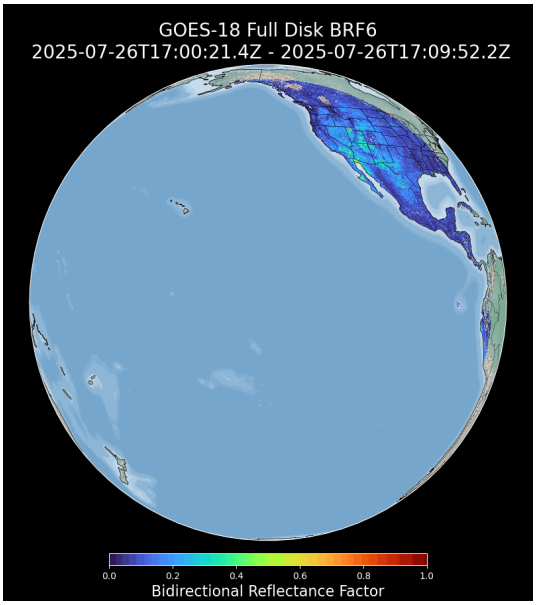

(e)

Figure 4.4 Plots of GOES-west Full Disk BRF (a) Band 1 (b) Band 2 (c) Band 3 (d) Band 5 (e) Band 6 on July 26, 2025 at 17:09 UTC.

4.2 Validation of the product

4.2.1 Datasets

4.2.1.1 Validated data

The validated data include the operational GOES-16 Full Disk data, GOES-17 Full Disk data, and GOES-18 Full disk data from June 17, 2022 to Oct 15, 2022. The data are sampled hourly.

4.2.1.2 Ground measurement of albedo

Ground reference data include: Ground measurements from networks including SURFace RADiation Budget (SURFRAD), Atmospheric Radiation Measurement at Southern Great Plains (ARM SGP) in situ observations (Table 4.2-4). The Surface Radiation Budget Network (SURFRAD), established in 1993, provides quality-controlled measurements of upwelling and downwelling shortwave radiation, direct and diffuse fraction as minute averages.

The Southern Great Plains (SGP) field measurement site established by the Atmospheric Radiation Measurement (ARM) user facility. Its intensive site distribution within SGP facilitates its advantage of comparing the data quality under similar environment conditions. Each site provides upward and downward shortwave radiation ground measurements.

Albedo is calculated as the ratio of outgoing and incoming solar irradiance. Incoming and outgoing shortwave radiation is measured at the ground sites and the instruments are well

maintained. The averages of albedo over 30 minutes are used to compare with instantaneous albedo retrieved by our algorithm. A standardized ground measurement data set reprocessed from original in-situ measurements with added cloud mask derived from downwelling shortwave radiation will be used in deriving the relevant reference data for comparison.

Table 4.1. Information of SURFRAD Stations

Site No.	Site Location	Latitude	Longitude	Surface types
1	Bondville, IL	40.05	-88.37	Crop
2	Desert Rock, NV	36.63	-116.02	Open shrub
3	Fort Peck, MT	48.31	-105.10	Grass
4	Goodwin Creek, MS	34.25	-89.87	Deciduous Forest
5	Pennsylvania State University, PA	40.72	-77.93	Mixed Forest
6	Sioux Falls, SD	43.73	-96.62	Forest

Table 4.2. Information of ARM-SGP Stations

Facility Name	Latitude	Longitude	Surface Type
sgpsirsC1	36.605	-97.485	Rangeland
sgpsirsE9	37.133	-97.266	Pasture
sgpsirsE11	36.881	-98.285	Pasture
sgpsirsE12	36.841	-96.427	Native Prairie
sgpsirsE13	36.605	-97.485	Pasture and Wheat
sgpsirsE15	36.431	-98.284	Pasture
sgpsirsE21	35.615	-96.065	Forest
sgpsirsE31	37.151	-98.362	Pasture
sgpsirsE32	36.819	-97.82	Pasture
sgpsirsE33	36.926	-97.082	Cultivated field to south, site in grassy field
sgpsirsE34	37.069	-96.761	Pasture
sgpsirsE35	35.862	-97.07	Pasture
sgpsirsE36	36.117	-97.511	Pasture
sgpsirsE37	36.311	-97.928	Cultivated field to south, site in grass
sgpsirsE38	35.88	-98.173	Cultivated field to south, site in grass

sgpsirsE39	36.374	-97.069	Cultivated field to south, site in grass
sgpsirsE40	36.319	-96.762	Pasture
sgpsirsE41	36.88	-97.086	Cultivated field to south, site in grass

4.2.1.3 **Ground surface reflectance.**

Based on the ancillary information on aerosol and water vapor from the Aerosol Robotic Network (AERONET) sites, a set of surface albedo and reflectance data is retrieved. The AERONET is a global aerosol observation network to provide ground-based remote sensing aerosol estimations. Five specific measurements from AERONET are used: the AOD measured at 500-nm, AOD measured at 675-nm, and Precipitable Water Vapor (PWV), Ozone, and refractive indices for aerosols. The AERONET data would be matched with the GOES-R Series BRF product in timestamps. Then the satellite TOA reflectance and the ground measurements listed in description are used as input to the 6S (Second Simulation of a Satellite Signal in the Solar Spectrum, Vector) radiative transfer model to calculate the reference BRF and compare with the satellite retrievals.

4.2.2 **Validation Results of albedo**

Generally, the retrieved albedo values align well with field measurements. Our retrieval algorithm requires a shorter compositing window, which enables it to better capture rapid surface dynamics when ABI data are available.

The overall comparison result of G16 LSA is as expected. It shows high consistency with the ground albedo values, although the satellite retrieval indicates a minor overestimation of about 0.0232, with a precision of about 0.0231. The overall comparison result of G17 LSA is similar to G16, although retrieving BRDF over land surfaces from G17 data is more challenging due to the larger VZA angle. The G18 LSA and the G17 LSA demonstrate high consistency with ground albedo values. For all three satellites, 100% of the matchups fall within the valid range defined by the accuracy and precision requirements.

The time series results illustrated in Figures 4.8 and 4.9 from the SURFRAD and ARM-SGP sites show that the GOES-R albedo corresponds with the ground diurnal variation.

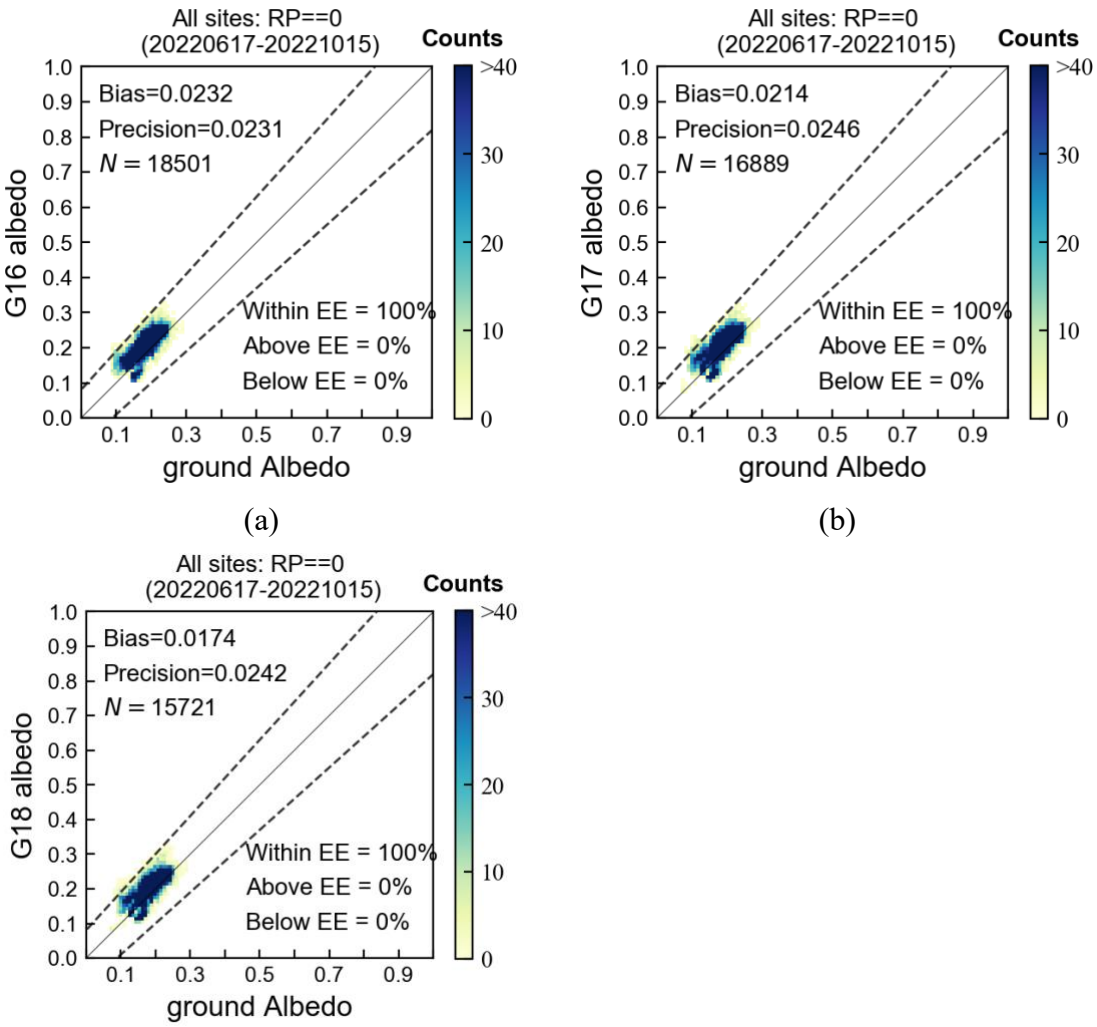

Figure 4.7 Scatter Plots from comparison between the GOES-16 and GOES-17 LSA and ground measurements over SURFRAD and ARM-SGP sites. (a) G16 high-quality vs. Ground; (b) G17 high-quality vs. Ground; (c) G16 medium-quality vs. Ground.

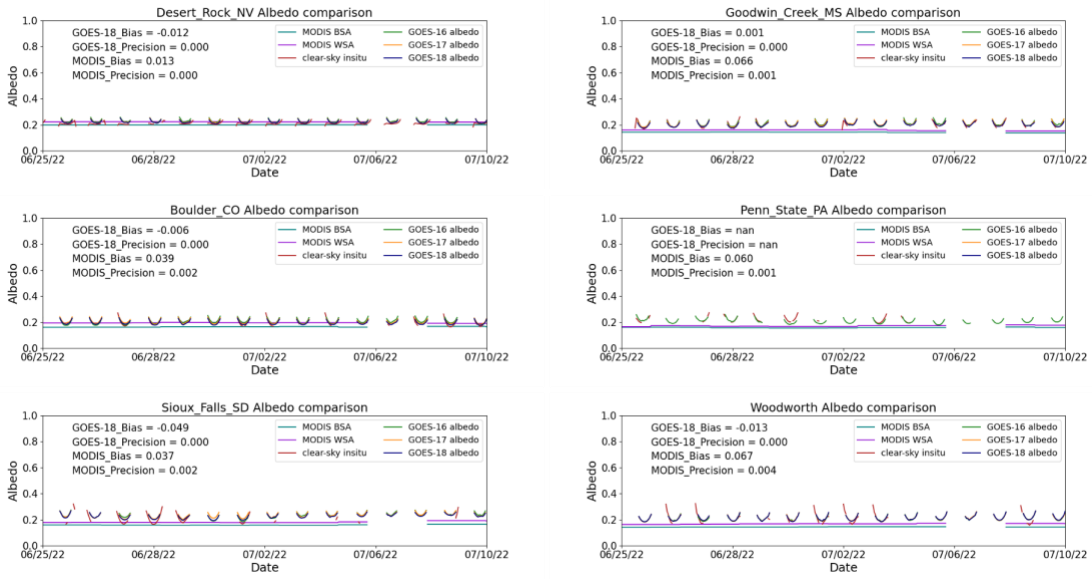

Figure 4.8 Time-series comparison between the GOES series LSA and ground measurements over SURFRAD sites.

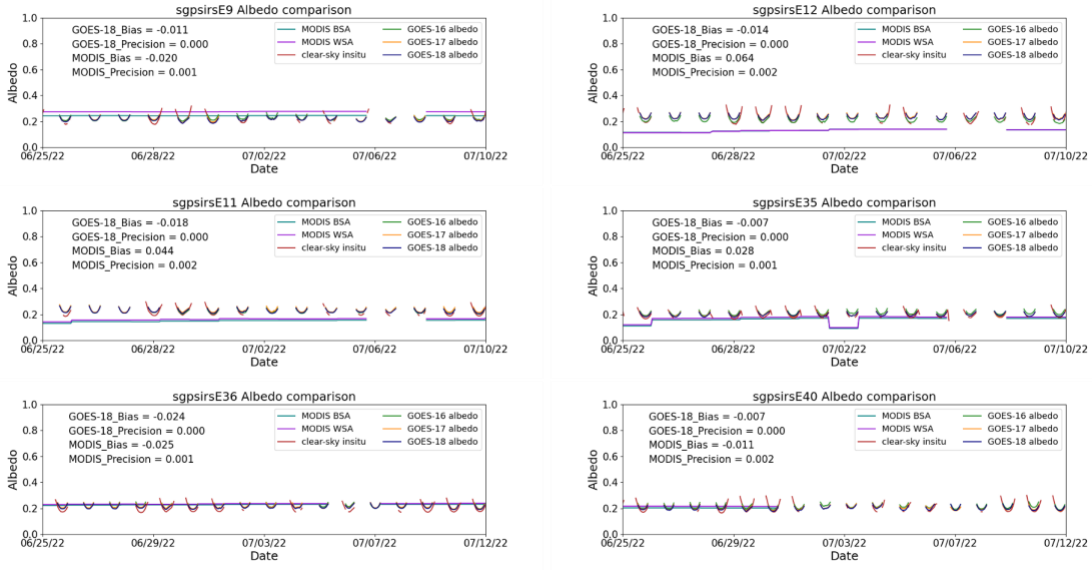

Figure 4.9 Time-series comparison between the GOES series LSA and ground measurements over ARM-SGP sites.

In some relatively heterogeneous sites such as Bondville and Sioux_falls, the GOESR LSA shows an over-estimation, which is related the surface heterogeneity, meaning the insitu value and the satellite pixel observe range difference has caused this bias. These two sites are crop covered. There are many farmland plots within the pixel range. The crop growth status various from plot to plot. Thus, the albedo values within the instrument view and the pixel view show seasonal difference. Also, the Sioux_Fall_SD site has covered some artificial bright surface, which has increased the difference. The scale difference has been assessed using a high-resolution albedo derived from Landsat 8 OLI data shown in Figure

4.10. The scale difference is defined as the difference between site albedo and pixel albedo both aggregated from Landsat-8 30-m spatial resolution data.

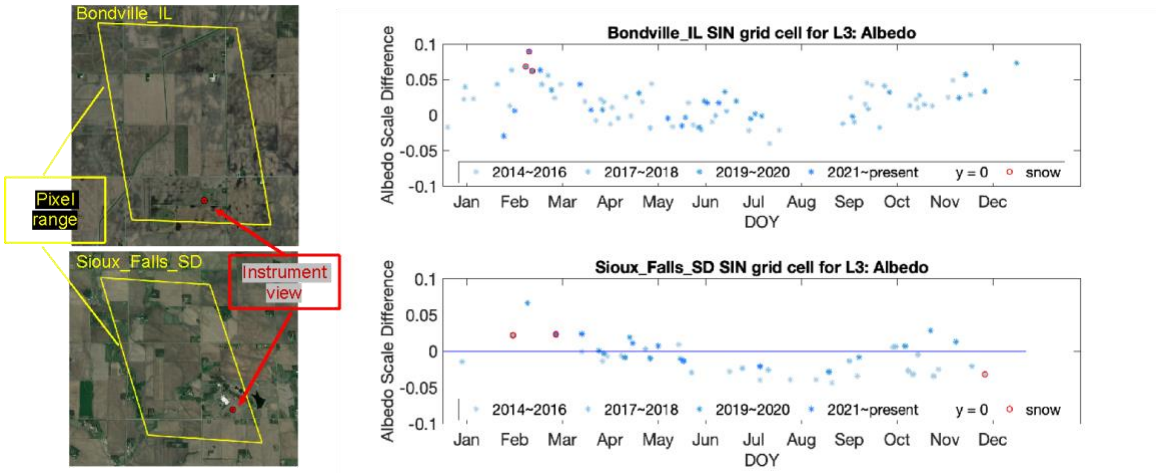

Figure 4.10 Time-series albedo scale difference between the GOES-16 pixel and ground instruments.

4.2.3 **Validation results of BRF**

In the validation of BRF, we deploy the AERONET network ground measurements including AOD, water vapor, ozone, and refractive indices for aerosols to determine the AOD profile. The radiative transfer approach is also independent, while the reference value is from 6S and our LUT is from Modtran.

The general premise behind this approach is to compare the surface reflectance derived from atmospheric correction using the image parameters against the equivalent using the station derived parameters. This assumes that the surface reflectance derived from the ground parameters is the “truth”

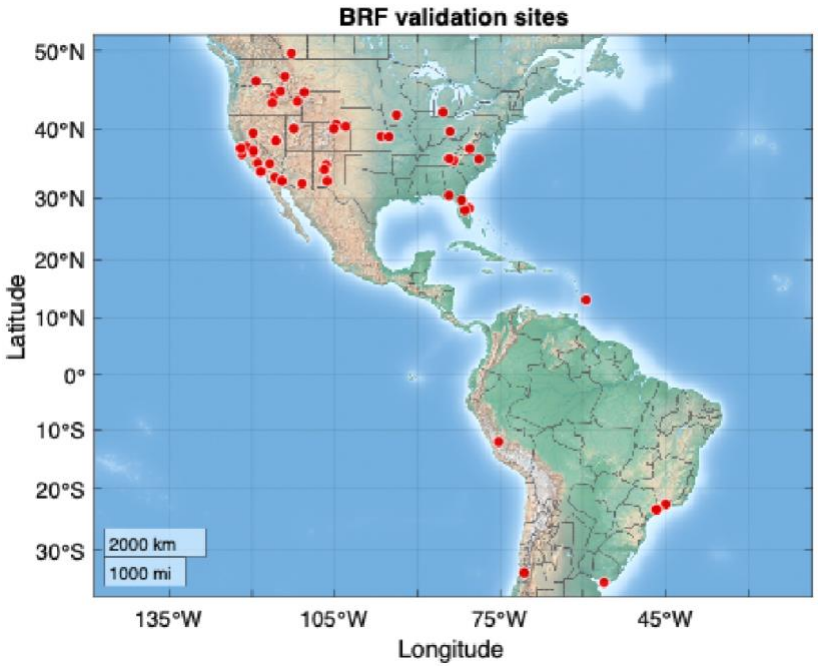

Figure 4.11 Site distribution of the selected AERONET sites used in the evaluation.

AERONET sites were selected for validating the surface reflectance results shown in Figure 4.11, with the comparison results presented in Figures 4.12–4.14. Corresponding statistical summaries are provided in Table 4.4. The retrieved surface reflectance across the five bands effectively captures the seasonal patterns and aligns closely with AERONET instantaneous reflectance measurements. Given the diverse surface cover types at these sites, the results demonstrate the proposed algorithm's capability to accurately handle varying land cover conditions, irrespective of homogeneity.

The validation results of the G16 BRF product from June show strong agreement with reference values across all channels. Channel 1 is notably more sensitive to aerosol optical depth (AOD) and thus requires additional consideration.

Similarly, the G19 BRF product shows good agreement with independent reference data, maintaining consistent performance comparable to the G18 results in both the FD (Figure 4.13) and CONUS (Figure 4.14) products.

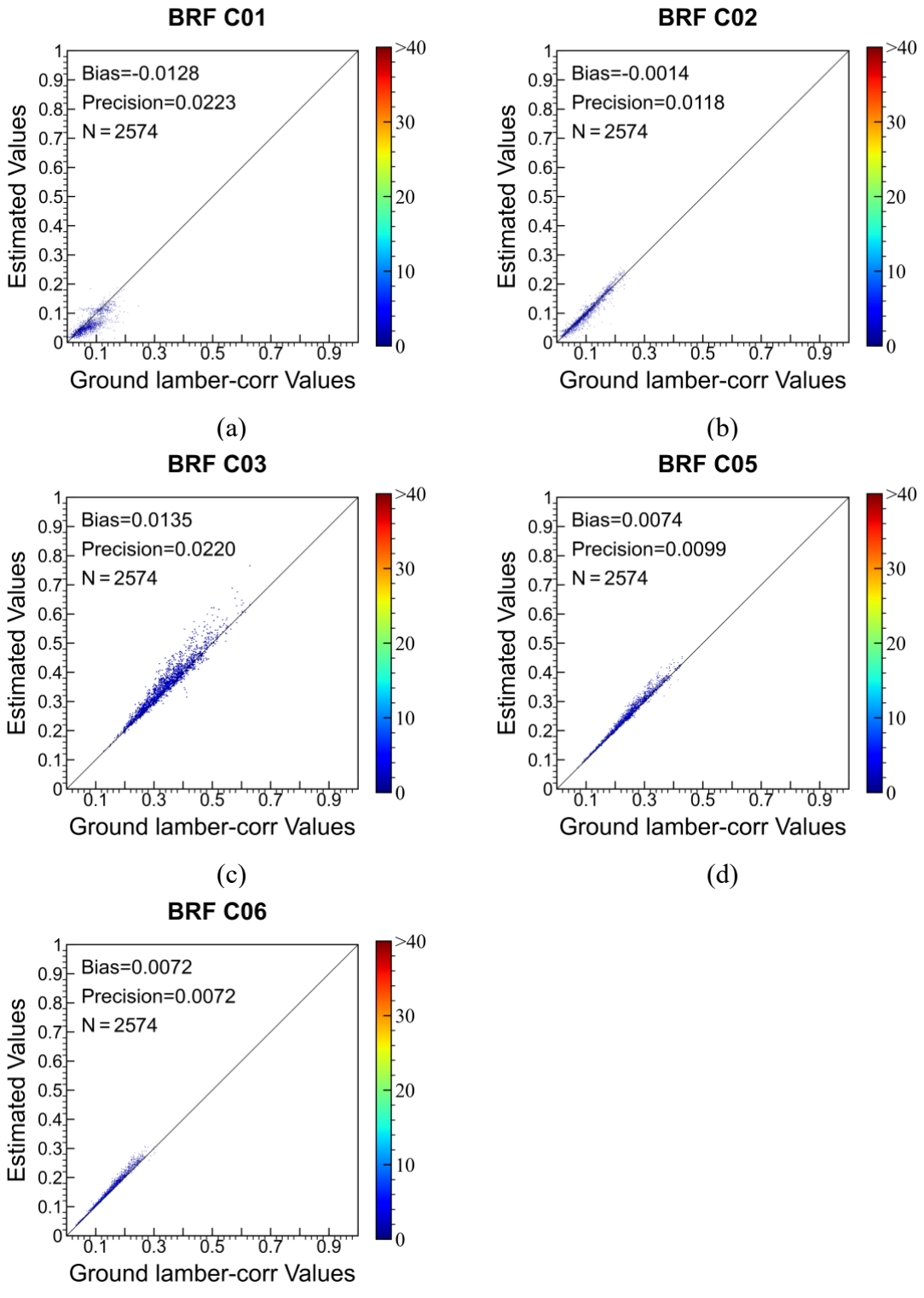

Figure 4.12 Comparison between GOES-R G16 FD BRF with surface reflectance atmospherically corrected using AERONET ground measurements from Jun 5, 2021 to Jul 3, 2021

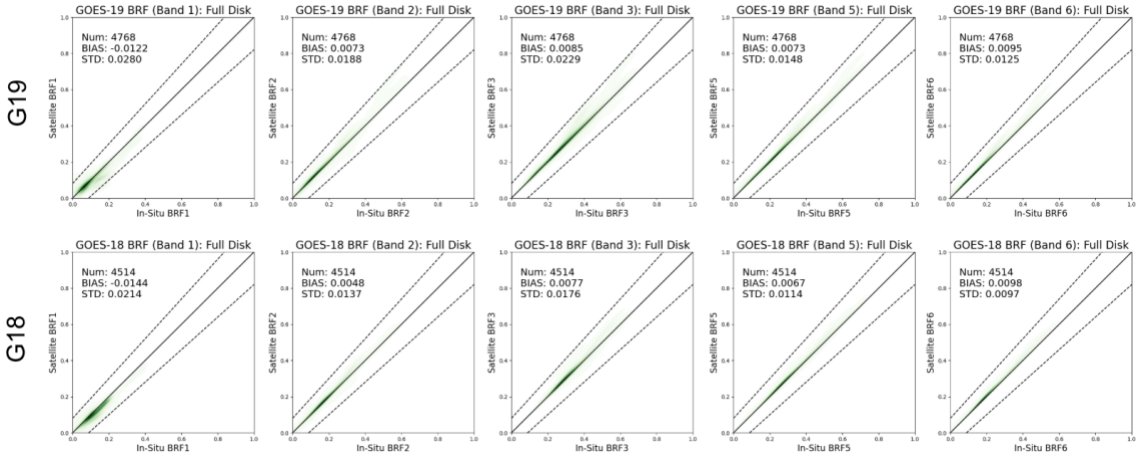

Figure 4.13 Comparison between GOES-19 FD BRF (up) and GOES-18 FD BRF (down) with surface reflectance atmospherically corrected using AERONET ground measurements from October 2, 2024 to February 1, 2025.

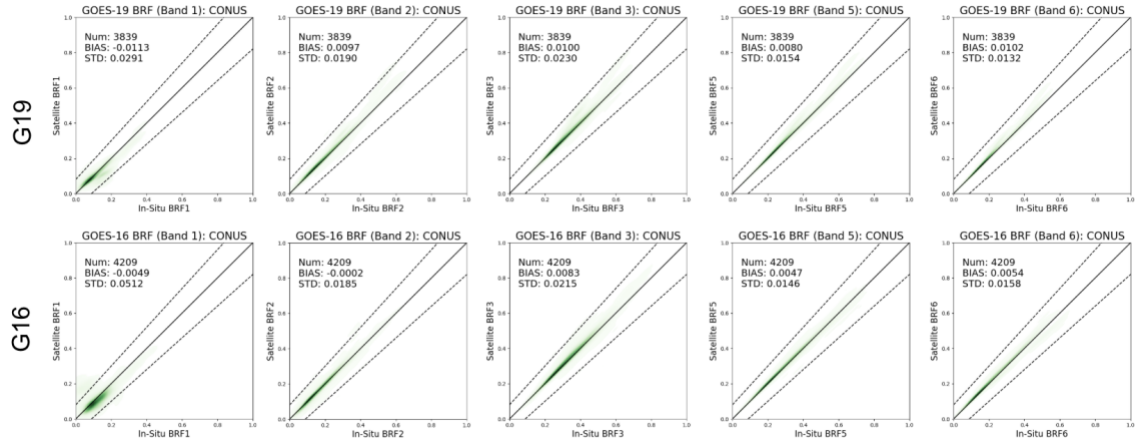

Figure 4.14 Comparison between GOES-19 FD BRF (up) and GOES-18 CONUS BRF (down) with surface reflectance atmospherically corrected using AERONET ground measurements from October 2, 2024 to February 1, 2025.

5 PRACTICAL CONSIDERATIONS

5.1 Numerical Computation Considerations

Accurate retrieval of albedo requires reliable acquisition of atmospheric parameters. Forward running of atmospheric radiative transfer model is time-consuming and not suitable for operational retrieval of albedo. Instead, the LSA algorithm pre-runs the atmospheric radiative transfer at some given conditions and stores the parameters into the LUTs to save computational time.

The current version of the LSA algorithm includes an optimization process. To speed up the iterative process, we may have to limit the number of iterations or adjust the iteration convergence criteria. Moreover, the optimization procedure takes advantage of multiple processor cores to perform parallel block processing on large FD image to reduce the latency. The default number of processes is 24.

5.2 Programming and Procedural Considerations

The LSA algorithm is purely a pixel-by-pixel algorithm. However, it requires a time series of clear-sky observations to achieve enough information to inverse BRDF models. Given the data volume of full disk albedo products, it is inefficient to gather a stack time series data over all pixels at each ABI scanning time. Given that the BRDF parameters do not vary greatly over a short period of time, we use the pre-calcualted BRDF parameters from the previous day to save computational time. In order to achieve this, we divide our algorithm into two parts, online and offline modes, respectively.

5.3 Quality Assessment and Diagnostics

The retrieval process of albedo will be monitored and the retrieval quality will be assessed. A set of quality flags and metadata will be generated with the albedo product for retrieval diagnostics. These flags will indicate the retrieval conditions, including the land/water mask, solar zenith angle and local zenith angle ranges. These flags also indicates the data quality (Is the data quality of AOD available? Is a routine BRDF retrieval algorithm successful? Which path is used to calculate LSA and BRF). The detailed information is documented in Section 3.5.

5.4 Exception Handling

The LSA algorithm checks for conditions where the albedo retrieval cannot be performed. These conditions include the failure of sensors, such as saturated channels or missing values. They also include the conditions when continuous clouds are present so that there are no enough clear-sky observations. However, the LSA algorithm tries to avoid using filling values if possible, in order to produce continuous and consistent products. The LSA algorithm selects various paths to calculate albedo and BRF in the online mode. The filling

value of BRF is used only when no BRDF parameter is retrieved and the current observation is cloudy. The LSA algorithm cannot run without cloud mask. However, if there is no AOD available, the offline mode is still able to run normally and the online mode will use a default AOD value to calculate diffuse irradiance ratio and carry out atmospheric correction.

5.5 Algorithm Validation

A summary of our previous validation results has been given in Section 4. The LSA/BRF validation strategy is to assess the error sources in the product via comparison with ground truth or inter-comparison with similar satellite products.

5.5.1 Inspection

Automated processing determines if all valid retrieval values from the three (FD, CONUS, and mesoscale) LSA/BRF products are within the required LSA/BRF retrieval range.

5.5.2 Routine Analysis

The Local Monitoring and Ground Validation Tool Set will be used to routinely acquire LSA matchup data sets with in-situ cloud filtering, and to make comparisons between satellite and ground stations. A separate BRF Validation Tool will be used to acquire BRF matchup date sets between satellite and ground derived counterparts.

5.5.2.1 LSA Monitoring

Effective cloud screening is required in the validation attempts considering significant contrast between cloud albedo and surface albedo. A cloud mask algorithm based on time series of in situ downward shortwave radiation as input was developed for an extra cross reference for the cloud filtering.

Procedures used in automatic direct comparison with in situ measurements include the following: Procedures and approaches used in direct validation include acquisition of ground measurements as ground truth. At the current 2-km scale, direct radiation measurements from pyranometers are recommended over relatively homogeneous pixels, while the homogeneity will be evaluated through other high resolution albedo/reflectance products, such as Landsat at 20-m resolution. The direct comparison provides an evaluation metric of the product performance. The accuracy and precision specifications for the FD product are the same as for the CONUS, and similar validation procedures will be applied to it.

Procedures and approaches used in manual inter-comparison include the following: Given existing GOES-R Series albedo products or similar satellite products such as MODIS BRDF-derived albedo/reflectance, data difference in spatial and temporal characteristics is observed when assessing product accuracy and consistency.

Direct comparison statistics from each in situ site will be generated throughout the validation as routine monitoring output. Changes that appear in the routine report of observed differences between satellite and surface LSA that exceed the threshold will serve as an "early warning" indicator of problems that warrant deep dive analysis.

5.5.2.2 BRF Monitoring

Automatic direct comparison of GOES-R Series BRF with in situ measurements requires periodical downloading of the latest ground measurements, extracting of the satellite BRF data and TOA reflectance, calculating reference BRF value using ground measurements and doing the analysis. The accuracy and precision specifications for the FD product are the same as for the CONUS, and similar validation procedures will be applied to it.

Direct comparison statistics from each in situ site will be generated throughout the validation as routine monitoring output as an evaluation metric of the product performance. Abnormal differences between satellite and surface BRF that exceed the threshold will serve as an "early warning" for further attention and deep analysis.

5.5.3 **Deep Dive Analysis**

Deep dive analysis will be conducted when a more detailed analysis is warranted based on routine monitoring results; however, deep-dive processes are mostly geared toward calibrating for algorithm coefficients and testing of different retrieval algorithm(s) for potential algorithm improvement. The deep-dive analysis will accomplish detailed point analyses on LSA seasonal trends.

5.6 Performance

The following assumptions have been made in developing and estimating the performance of the ABI LSA algorithm:

- Surface BRF is modeled by the revised linear kernel function with three coefficients.
- Surface anisotropy is constant within days through a moving window and can be represented by the linear kernel model.
- The reciprocity principle is valid at ABI resolutions.
- The systematic bias caused by lambertian assumption is acceptable. It is assumed to cause an underestimation of surface reflectance when BRDF is high and overestimation when BRDF is low.

5.7 Assumed Sensor Performance

The ABI LSA algorithm requires a time series of clear sky TOA reflectance inputs. The number of clear sky observations within a short time period will influence the retrieval quality of LSA and corresponding land surface reflectance by-products. Additionally, the algorithm relies on the cloud mask product to distinguish clear-sky observations from cloud sky observations. The retrieval accuracy also depends on the quality of cloud mask.

5.8 Algorithm Improvement

The introduction of prior knowledge such as the aerosol types, BRDF models, BRDF climatology, and albedo climatology will improve the retrieval quality of LSA and land surface reflectance. Currently, we use the multi-year's mean and variance of MODIS albedo products as one of the constraints in our optimization code. We are currently working on analyzing more existing satellite albedo/BRDF products and in an effort to incorporate as much background knowledge as possible. Moreover, we are considering to develop an AOD climatology for improving the offline optimization efficiency and online albedo and reflectance accuracy.

6 REFERENCES

Chen, Y.M., Liang, S., Wang, J., Kim, H.Y., & Martonchik, J.V. (2008). Validation of MISR land surface broadband albedo. *International Journal of Remote Sensing, 29*, 6971-6983

Duan, Q.Y., Gupta, V.K., & Sorooshian, S. (1993). Shuffled complex evolution approach for effective and efficient global minimization. *Journal of Optimization Theory and Applications, 76*, 501-521

Duan, Q.Y., Sorooshian, S., & Gupta, V. (1992). Effective and efficient global opitimization for conceptual rainfall-runoff models. *Water Resources Research, 28*, 1015-1031

Govaerts, Y.M., Wagner, S., Lattanzio, A., & Watts, P. (2010). Joint retrieval of surface reflectance and aerosol optical depth from MSG/SEVIRI observations with an optimal estimation approach: 1. Theory. *Journal of Geophysical Research-Atmospheres, 115*

He, T., Liang, S.L., Wang, D., Wu, H., Yu, Y., & Wang, J. (2012). Estimation of surface albedo and directional reflectance from Moderate Resolution Imaging Spectroradiometer (MODIS) observations. *Remote Sensing of Environment, 119*, 286-300

He, T., Zhang, Y., Liang, S., Yu, Y., & Wang, D. (2019). Developing Land Surface Directional Reflectance and Albedo Products from Geostationary GOES-R and Himawari Data: Theoretical Basis, Operational Implementation, and Validation. *Remote Sensing, 11(22), 2655.*

Liang, S., Yu, Y., & Defelice, T.P. (2005a). VIIRS narrowband to broadband land surface albedo conversion: formula and validation. *International Journal of Remote Sensing, 26*, 1019-1025

Liang, S.L. (2001). Narrowband to broadband conversions of land surface albedo I Algorithms. *Remote Sensing of Environment, 76*, 213-238

Liang, S.L. (2003). A direct algorithm for estimating land surface broadband albedos from MODIS imagery. *Ieee Transactions on Geoscience and Remote Sensing, 41*, 136-145

Liang, S.L. (2004). *Quantitative remote sensing of land surfaces*. Hoboken, New Jersey: John Wiley & Sons, Inc

Liang, S.L., Fang, H.L., Chen, M.Z., Shuey, C.J., Walthall, C., Daughtry, C., Morisette, J., Schaaf, C., & Strahler, A. (2002). Validating MODIS land surface reflectance and albedo products: methods and preliminary results. *Remote Sensing of Environment, 83*, 149-162

Liang, S.L., Shuey, C.J., Russ, A.L., Fang, H.L., Chen, M.Z., Walthall, C.L., Daughtry, C.S.T., & Hunt, R. (2003). Narrowband to broadband conversions of land surface albedo: II. Validation. *Remote Sensing of Environment, 84*, 25-41

Liang, S.L., Strahler, A.H., & Walthall, C. (1999). Retrieval of land surface albedo from satellite observations: A simulation study. *Journal of Applied Meteorology, 38*, 712-725

Liang, S.L., Stroeve, J., & Box, J.E. (2005b). Mapping daily snow/ice shortwave broadband albedo from Moderate Resolution Imaging Spectroradiometer (MODIS): The improved direct retrieval algorithm and validation with Greenland in situ measurement. *Journal of Geophysical Research-Atmospheres, 110*

Maignan, F., Breon, F.M., & Lacaze, R. (2004). Bidirectional reflectance of Earth targets: Evaluation of analytical models using a large set of spaceborne measurements with emphasis on the Hot Spot. *Remote Sensing of Environment, 90*, 210-220

NOAA (2009). GOES-R Series Ground Segment Project Functional and Performance Specification. In

Pinty, B., Roveda, F., Verstraete, M.M., Gobron, N., Govaerts, Y., Martonchik, J.V., Diner, D.J., & Kahn, R.A. (2000a). Surface albedo retrieval from Meteosat - 1. Theory. *Journal of Geophysical Research-Atmospheres, 105*, 18099-18112

Pinty, B., Roveda, F., Verstraete, M.M., Gobron, N., Govaerts, Y., Martonchik, J.V., Diner, D.J., & Kahn, R.A. (2000b). Surface albedo retrieval from Meteosat - 2. Applications. *Journal of Geophysical Research-Atmospheres, 105*, 18113-18134

Qin, W.H., Herman, J.R., & Ahmad, Z. (2001). A fast, accurate algorithm to account for non-Lambertian surface effects on TOA radiance. *Journal of Geophysical Research-Atmospheres, 106*, 22671-22684

Schaaf, C., Martonchik, J., Pinty, B., Govaerts, Y., Gao, F., Lattanzio, A., Liu, J., Strahler, A., & Taberner, M. (2008). Retrieval of Surface Albedo from Satellite Sensors. In S. Liang (Ed.), *Advances in Land Remote Sensing: System, Modeling, Inversion and Application* (pp. 219-243). New York: Springer

Schaaf, C.B., Gao, F., Strahler, A.H., Lucht, W., Li, X.W., Tsang, T., Strugnell, N.C., Zhang, X.Y., Jin, Y.F., Muller, J.P., Lewis, P., Barnsley, M., Hobson, P., Disney, M., Roberts, G., Dunderdale, M., Doll, C., d'Entremont, R.P., Hu, B.X., Liang, S.L., Privette, J.L., & Roy, D. (2002). First operational BRDF, albedo nadir reflectance products from MODIS. *Remote Sensing of Environment, 83*, 135-148

Wagner, S.C., Govaerts, Y.M., & Lattanzio, A. (2010). Joint retrieval of surface reflectance and aerosol optical depth from MSG/SEVIRI observations with an optimal estimation approach: 2. Implementation and evaluation. *Journal of Geophysical Research-Atmospheres, 115*

Wang, D., Liang, S.L., He, T., & Yu, Y. (2013). Direct estimation of land surface albedo from VIIRS data: algorithm improvement and preliminary validation. *Journal of Geophysical Research-Atmospheres, 118*, 12,577-512,586

Wang, Y.J., Lyapustin, A.I., Privette, J.L., Morisette, J.T., & Holben, B. (2009). Atmospheric Correction at AERONET Locations: A New Science and Validation Data Set. *Ieee Transactions on Geoscience and Remote Sensing, 47*, 2450-2466

Yang, F.L., Mitchell, K., Hou, Y.T., Dai, Y.J., Zeng, X.B., Wang, Z., & Liang, X.Z. (2008). Dependence of Land Surface Albedo on Solar Zenith Angle: Observations and Model Parameterization. *Journal of Applied Meteorology and Climatology, 47*, 2963-2982